Desalination and Water Treatment
www.deswater.com

doi: 10.1080/19443994.2014.995140

57 (2016) 4269–4295
February

Taylor & Francis
Taylor & Francis Group

The forward osmosis and desalination

M.A. Darwish, H.K. Abdulrahim*, A.S. Hassan, A.A. Mabrouk, A.O. Sharif

Qatar Environment and Energy Research Institute, Qatar Foundation, PO Box 5825, Doha, Qatar, Tel. +974 44545880; email: madarwish@qf.org.qa (M.A. Darwish), Tel. +974 44545884; email: habdelrehem@qf.org.qa (H.K. Abdulrahim), Tel. +974 44545887; email: ahassan@qf.org.qa (A.S. Hassan), Tel. +974 44547453; email: aaboukhlewa@qf.org.qa (A.A. Mabrouk), Tel. +974 44546431; email: asharif@qf.org.qa (A.O. Sharif)

Received 23 July 2014; Accepted 24 November 2014

ABSTRACT

Forward osmosis (FO) has emerged as a method for desalting saline water and power production. It utilizes a chemical potential difference, or a salinity gradient to permeate fresh water through membranes. This paper investigates the feasibility of using the FO process for seawater (SW) desalination in terms of consumed energy, capital costs, water recovery, operation & maintenance, water quality, and the final product water cost. The study covers FO by itself, and when combines with other desalting systems such as reverse osmosis, multi stage flash (MSF), and multi effect distillation as pretreatment method. This paper reviews first the principles of fluid and solutes flow in the FO membranes, concentration polarization, the difference between the FO, pressure retarded osmosis processes, draw solutions, and the solutes involved in these draw solutions. Then, the main characteristics of the FO membranes and their commercial availability are presented. Previous experimental work and a commercial plant using FO for desalination are also given. The use of FO as pretreatment for other desalting methods is presented in light of two proposed research projects. The first research project proposes utilizing FO as pretreatment for processing treated wastewater and SW in one system. The second project utilizes FO as pretreatment for a once-through MSF desalting method. The analysis proved energy reduction in the energy consumption of both desalting systems by more than 50 and 18%, respectively.

Keywords: Forward osmosis; Reverse osmosis; Once-through MSF; Concentration polarization; Draw solution

1. Introduction

Development of low-cost seawater (SW) desalination technology is essential for countries like Qatar, where desalted seawater (DW) represents almost 99% of the municipal water supply. Seawater reverse osmosis (SWRO) desalting systems are presently the least cost, most energy efficient, and most commonly used worldwide to produce DW. Reverse osmosis (RO) is a membrane separation process, shown in Fig. 1. Almost pure water is permeated from the saline feed water (e.g. SW) when it is pumped against a semi-permeable membrane side at a pressure higher than the SW osmotic pressure. This forces almost pure water, but not solutes, to pass through the membrane. The RO process consumes much less energy than the two extensively used thermal desalting methods in

*Corresponding authors.

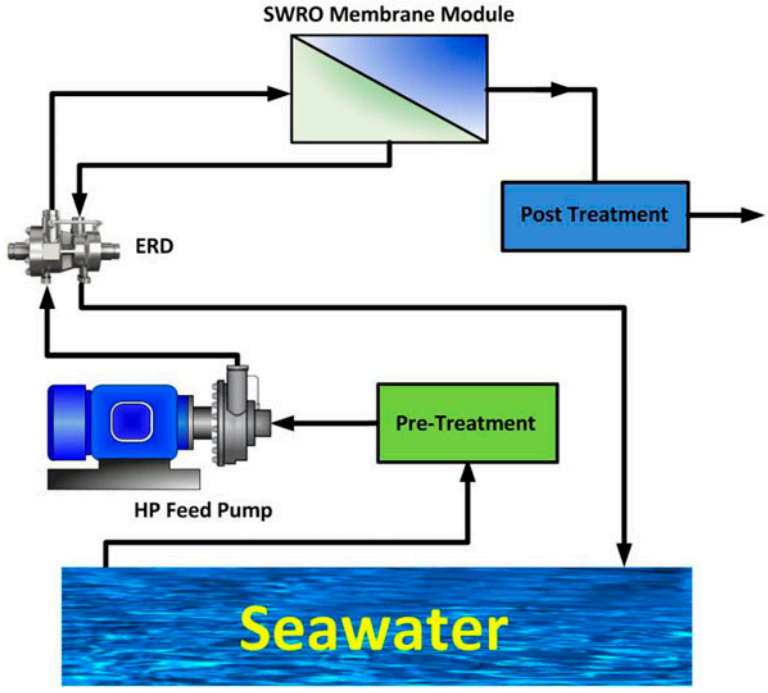

Fig. 1. Schematic diagram of RO desalting system.

Qatar and other Gulf Co-operation Countries (GCC), namely (a) multi stage flash (MSF) and (b) multi effect distillation–thermal vapor compression (MED–TVC) desalting methods. However, the RO is still considered an energy-intensive process because of the high hydraulic pressure required to overcome the osmotic pressure (π) of SW. Other problems in RO include membrane fouling and low recovery ratio (permeate to feed ratio).

Forward osmosis (FO) method is an emerging saline water desalting process. It is claimed that the FO process has some advantages compared with RO system such as high rejection of contaminants, low membrane fouling, and less consumed energy [1,2]. The questions raised about the FO are: can the FO really compete with the SWRO system; or at least can it reduce the SWRO consumed energy (and thus the water cost) when the FO is combined with the RO system.

FO is an osmotic process, like RO system. In FO, a semi-permeable membrane separates a draw solution having high osmotic pressure π_D from saline feed water having dissolved solutes such as SW of low osmotic pressure π_F, compared to π_D. The subscript F and D stands for the feed and draw solutions, respectively. The FO driving force is the water chemical potential (μ_w) difference between the feed saline water solution (of low π_F and high $\mu_{w,F}$) and the draw solution (of high π_D and low $\mu_{w,D}$), i.e.

$$\Delta\mu_w = \mu_{w,F} - \mu_{w,D} \quad (1)$$

The result of $\mu_{w,F} > \mu_{w,D}$ induces net water flow from the feed saline water (F) to the draw solution (D) without applying pressure on the saline water such as in the case of RO system, Fig. 2. Therefore, direct osmosis is the transport of water across a selectively permeable membrane from the feed solution of high chemical potential $\mu_{w,F}$ (low solute concentration or low π_F) to a draw solution of low chemical potential $\mu_{w,D}$, (high solute concentration and high π_D). It is driven by the solute concentration difference (ΔC_s) across the membrane that allows water passage, but not solutes. In Fig. 2 and the following text, the subscript w for water is omitted. Solutes are not supposed to pass through a semi-permeable membrane because the pore size of the membrane active layer is small enough to allow water molecules size only to pass, and not solutes. The resulted dilute draw solution is then separated to a product water and reconcentrated draw solution through a regeneration system.

The main characteristics required for an effective draw solution are:

- High solubility in water.
- High osmotic pressure π_D generated by the solute(s) in the solution to increase the flux across the membranes.

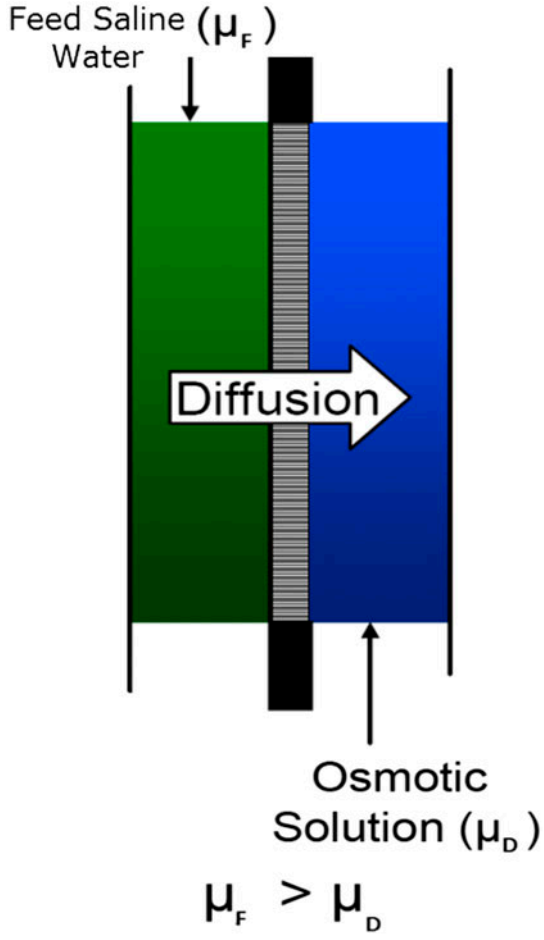

Fig. 2. Water flow across a semi-permeable membrane from feed saline water of high chemical potential μ_F (low salt concentration) to draw solution of low chemical potential μ_D (high salt concentration) [3].

- Low internal concentration polarization (ICP) (will be explained later).
- The solutes in the draw solution can be easily (and economically) separated to produce fresh water and to reconcentrate the draw solution for reuse.
- Low cost.
- No hazards.

The main characteristics required of the FO membrane are [2]:

- High-water permeability, typical high water transport coefficient (A) higher than 10×10^{-5} cm/s/bar.
- High solutes rejection, typical low salt transport coefficient (B) less than 0.21×10^{-5} cm/s.
- High value for the combination A^2/B, typically higher than 5.0×10^{-5} cm/s/bar^2
- Low ICP.
- High chemical stability and mechanical strength.

This paper studies the feasibility of using FO process for SW desalination in terms of consumed energy, capital costs, water recovery, operation and maintenance requirements, water quality, and the final product water cost when

(a) FO is used alone.
(b) FO is combined with other desalting systems such as RO, MSF, and MED as pretreatment.

Although the RO system is the most-used system for desalting SW, worldwide, the MSF and MED still are the most-used desalting systems in Qatar and other GCC countries. The present work introduces also a review on previous FO efforts for desalination, and challenges faced by the desalination by FO. These include:

(1) Investigating suitable draw agent with a reliable regenerating method.
(2) Structure and material of membrane/solution interface resulting from selective transfer of some species through the membrane under the effect of trans-membrane driving forces [4].
(3) Fouling and concentration polarization (CP) in the membrane.

2. CP in FO process

The accumulation of solutes close to the membrane is known as CP. The CP is a common and inevitable phenomenon in both pressure-driven and osmotic-driven membrane processes. In the RO process, the water flow through the membrane creates CP layer in the feed solution exposed to skin (dense layer). The concentration profile based on the one-dimensional flow assumption used in the unstirred film theory can be expressed by [5]:

$$C_{Fm} = C_{FB} \exp\left(\frac{J_w.\delta}{D}\right) \quad (2)$$

where J_w is the water flux across the membrane; volumetric flow rate per unit area, m/s; δ is the unstirred film thickness, m; and D is the diffusion coefficient of solute in water, m^2/s.

The CP is illustrated for the RO in Fig. 3(a) and (b), while the CP in FO is shown in Fig. 4. The flat-sheet RO membrane, as shown in the scanning electron microscope (SEM) image of Fig. 3(b), consists of thin, active semi-permeable membrane skin, (1.6-mil, 40-μm) membrane substructure, and a (2.7-mil, 70-μm) woven fabric backing [5]. In RO, the water flow creates minor CP on the exposed skin. The thickness of the support layer has no effect on the CP in the RO system, as shown in Fig. 3(b).

In the FO process, CP is created on both feed and draw solution sides of the membrane, Fig. 4, and not only the feed side as in the RO process. When RO membranes are used in the FO process, CPs are created upstream the active layer and inside and next to the supporting layer. The CP greatly reduces the effective osmotic pressure difference and "osmotic efficiency" of the process.

In Fig. 4, the CP at the active layer (C_{Fm}/C_{FB}) is called the *external* CP (ECP), and the CP (C_{Ds}/C_{Dm}) in the supporting layer is called ICP. Fig. 4 shows how ICP occurs in FO process when the feed solution is placed against the active thin layer. The effective concentration difference exists across the active layer of the

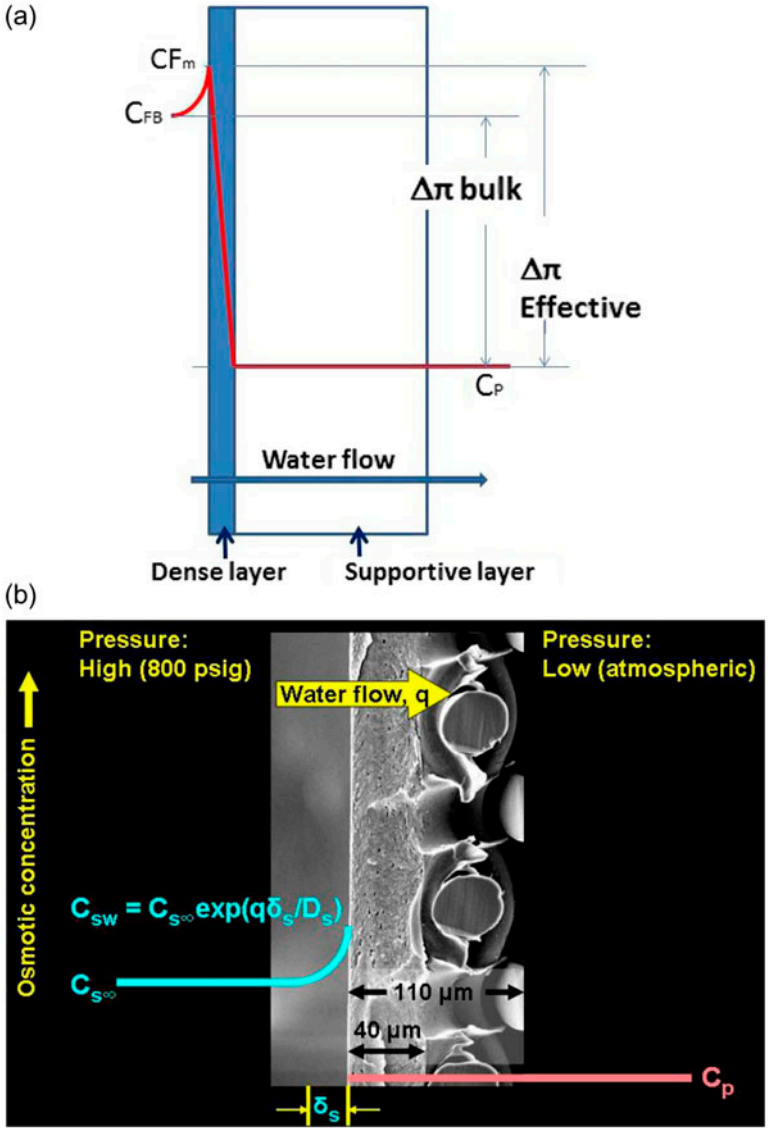

Fig. 3. (a) Schematic of RO concentration polarization illustrating how water flow causes the source solute (salt) concentration to increase near the membrane surface and (b) schematic of RO concentration polarization illustrating how water flow causes the source solute (salt) concentration to increase near the membrane surface, and shows a scanning electron microscope (SEM) image of a flat-sheet RO membrane [5].

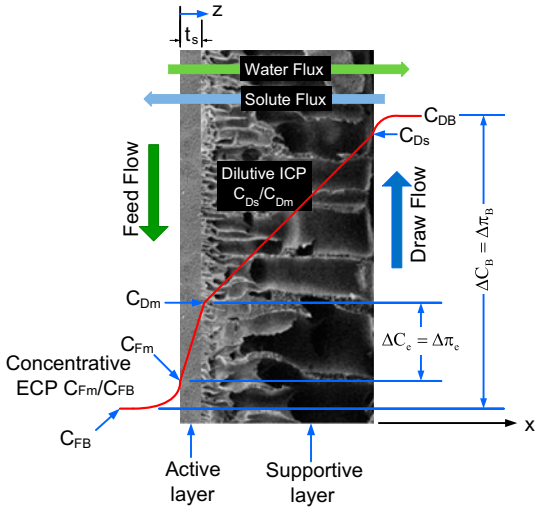

Fig. 4. Water flux and solute concentration profiles across a typical asymmetric or thin-film composite FO membrane.

membrane and is equal to ($C_{Dm} - C_{Fm}$), and is less than the bulk concentration difference ($C_{DB} - C_{FB}$). Thus, the effective chemical potential difference ($\pi_{Dm} - \pi_{Fm}$) is less than that of the bulk, i.e. ($\pi_{DB} - \pi_{FB}$) due to the effect of CP.

The general equation of water transport through a semi-permeable membrane in FO, pressure retarded osmosis (PRO) and RO is:

$$J_w = A\ (\sigma\Delta\pi - \Delta P) \tag{3}$$

The term J_w is the water flux across the membrane, A is the water permeability constant of the membrane and is proportional to the water diffusion coefficient in the membrane D_w and is inversely proportional to the membrane thickness t, σ presents the reflection coefficient, $\Delta\pi$ is the differential osmotic pressure, ΔP is the applied hydraulic pressure, and the difference ($\sigma\Delta\pi - \Delta P$) represents the effective driving force. The reflection coefficient σ represents salt-water coupling and can have values ranging from 0 to 1. When $\sigma = 0$ the membrane shows no salt rejection, when $\sigma = 1$ the membrane shows total salt rejection. For RO membranes with high salt rejection, σ approaches 1.

In water flow through a porous membrane (water diffusion), the water molecules have to overcome a tortuous path through the network of linked pores in order to render the real diffusion through the membrane. The corrective coefficient ε/τ was added to the thickness t, where ε is the membrane porosity, and τ is the path tortuosity factor.

In the FO process, no pressure is applied to the high concentration solution. Water flows from the low concentration side to the high concentration side. Therefore, in FO, ΔP is equal to zero. In a PRO process, pressure is applied on the high concentration solution, but it is less than the osmotic pressure difference across the membrane, and water flows also from low concentration side to high concentration side (as in FO). Therefore, in PRO, $\Delta\pi$ is more than ΔP.

In the RO process, the applied pressure on the high concentration solution is greater than the osmotic pressure difference across the membrane; and water flows from the high to low concentration sides. Therefore, in RO, ΔP is more than $\Delta\pi$. The flux directions of the permeating water in FO, PRO, and RO are illustrated in Fig. 5. The FO point, PRO zone, and RO zone, along with the flux reversal point, are illustrated in Fig. 6.

The water flux, J_w in liters per square meters per hour (L/m^{2}h) for the FO process ($\Delta p = 0$) can be described by the following equation:

$$J_w = A\sigma\Delta\pi \tag{4}$$

$$J_w = A\sigma(\pi_D - \pi_F) \tag{5}$$

$\Delta\pi$ is the osmotic pressure difference between the feed and draw solutions, i.e. ($\pi_D - \pi_F$).

The term $\Delta\pi$, in Eq. (4), should be applied across the membrane; it is the real driving force for the solvent (water) flow from feed solution to the draw solution. The draw solution has the high concentration solution (low water chemical potential) and the feed solution has the low concentration solution (high water chemical potential). Therefore, ($\pi_D - \pi_F$) should be the effective osmotic pressure difference in the membrane surfaces, namely,

$$J_w = A\sigma(\pi_{D,m} - \pi_{F,m}) \tag{6}$$

The solute concentrations can differ significantly at the membrane boundary layer as shown in Fig. 4 and the flow rate equation should be corrected to account for the ECP and ICP. In osmotic membrane processes, the CP is caused in general by the difference in concentration between the draw solution and the feed solution on both sides of the asymmetric membrane such as illustrated in Fig. 4. For FO, the ECP occurs at a solution layer next to the outer surface of the membrane selective layer (i.e. C_{Fm}/C_{FB} in Fig. 4), while the ICP in porous support layer is mainly C_{DB}/C_{Ds}.

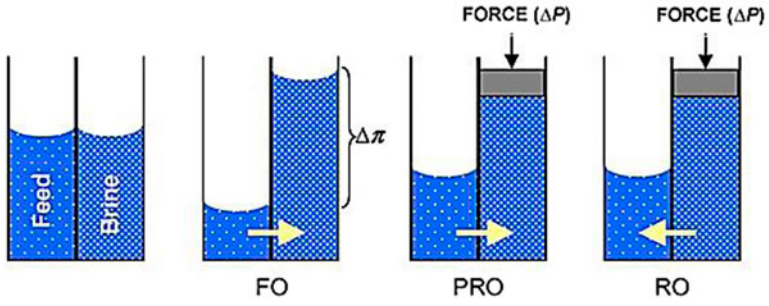

Fig. 5. Illustration of FO, PRO, and RO processes [1].

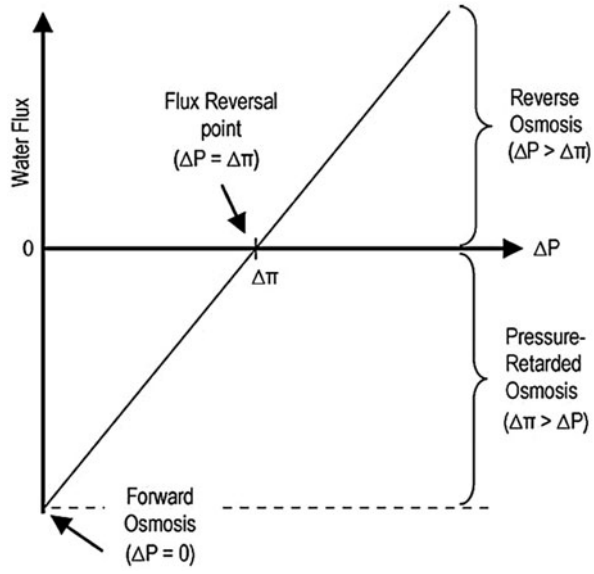

Fig. 6. Direction and magnitude of water flux as a function of applied pressure in FO, PRO, and RO [1].

When the feed is placed against the support layer of an asymmetric membrane (in PRO applications), Fig. 7(b), water enters the porous support layer and diffuses across the active layer into the draw solution. The *salt in the feed* freely enters the open structure as it is transported into this layer by convective water flow. This salt cannot easily penetrate the active layer from the support layer side and therefore increases the concentration within the porous layer. This is referred to as *concentrative ICP*. On the other hand, when the feed solution is against the active layer and the draw solution is against the backing layer, the ICP phenomenon now occurs on the permeate side. This is referred to as *dilutive ICP* since the draw solution is diluted by the permeate water within the porous support of the membrane. *Dilutive ICP* is illustrated in Fig. 7(a).

Similarly, concentrative ECP and dilutive ECP may exist depending upon the membrane orientation. *Concentrative ECP* occurs in the FO mode at the surface of the dense active layer of the membrane due to the rejected molecules near the membrane active layer on the feed side. It increases the effective feed osmotic pressure from π_{FB} to π_{Fm}. In FO, *dilutive ECP* occurs on the draw solution side, thus it can reduce the effective draw solution osmotic pressure from $\pi_{DB} \rightarrow \pi_{Ds}$, but this is usually negligible compared to the ICP.

The effect of ECP on permeate flux can be reduced by increasing flow turbulence. Unlike ECP, the ICP takes place within the porous support layer. It is the most troublesome phenomenon in FO processes because it cannot be eliminated easily. Therefore, the decline in water flux in FO is primarily caused by ICP and the flux can be reduced up to 80% [6].

The increased feed solute concentration at the membrane surface can lead to precipitation of sparingly soluble salts, scaling the membrane, and reducing water flux. The ICP occurs in the porous support layer of FO membranes due to solutes swept away from the backside of the membrane active layer by water diffusing through the membrane. Consequently, the osmotic pressure of the bulk draw solution is further reduced from π_{Ds} to π_{Dm} by ICP.

For ECP (C_{Fm}/C_{FB}), the general equation for CP modulus in pressure-driven membrane processes can be expressed as [6]:

$$\frac{C_{Fm}}{C_{FB}} = \exp\left(-\frac{J_w}{k}\right) \tag{7}$$

where k is called the mass transfer coefficient, and C_{Fm} and C_{FB} are the concentrations of the feed solution at the membrane. Since the concentration is relative, the previous equation can be expressed as [6]:

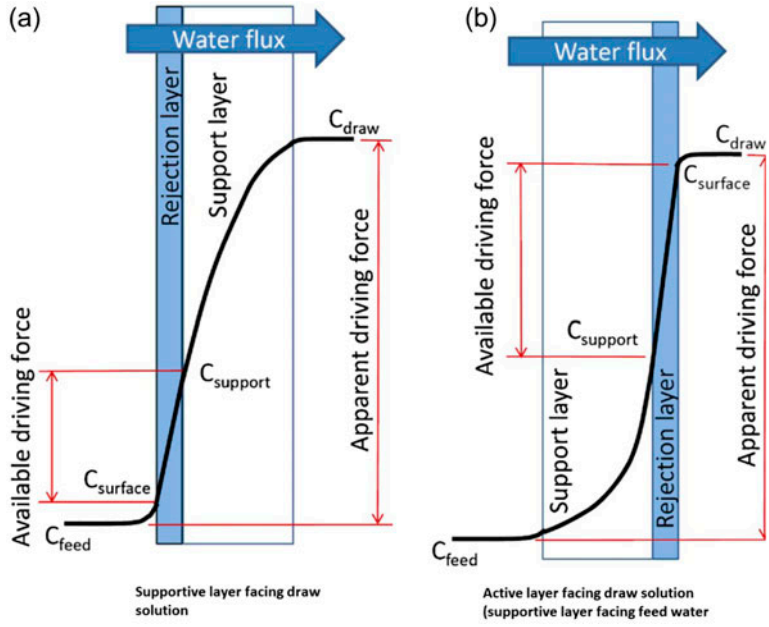

Fig. 7. Illustration of driving force and concentration polarization for (a) the FO mode and (b) the PRO mode. The ICP in (a) is called dilutive ICP, and in (b) concentrative ICP [7].

$$\frac{C_{Fm}}{C_{FB}} \cong \frac{\pi_m}{\pi_B} = \exp\left(-\frac{J_w}{k}\right) \tag{8}$$

where π_m and π_B are the osmotic pressures of the feed solution at the membrane surface and in the bulk, respectively.

Hence, the equation for J_w (considering ECP alone while neglecting ICP), may be given by [6]:

$$J_w = A\left[\pi_{D,B}\exp\left(-\frac{J_w}{k_D}\right) - \pi_{F,B}\exp\left(-\frac{J_w}{k_F}\right)\right] \tag{9}$$

The mass transfer coefficient (k) is related to the Sherwood number (Sh) by,

$$k = \frac{\mathrm{Sh}\cdot D}{D_h} \tag{10}$$

The following points are noticed in (Eq. 9):

- This model is only suitable for a dense symmetric film, and not for an asymmetric membrane. Therefore, the application of this model is relatively limited. The situation of an asymmetric FO membrane is used in practice where ICP effects are more important.
- The mass transfer coefficients on the feed and draw solution sides are not the same because of the concentration gradient.
- It is assumed that the solute permeability coefficient is zero (i.e. reflection coefficient $\sigma = 1$).
- The feed and draw solution concentrations are relatively low, and their ratio is almost equal to their osmotic pressure ratio.

The ICP is one of the most important phenomena in osmotic-driven membrane processes. It has been recognized that the water flux decline in FO is predominantly caused by ICP. Early FO studies showed that ICP could significantly reduce the water flux. Two types of ICP, namely the dilutive ICP and concentrative ICP, can occur within the membrane support layer depending upon the membrane orientation as illustrated in Fig. 7. The problem of ICP within the support layer is that it cannot be mitigated by increasing the flow rate or turbulence as ECP.

2.1. Mass transfer equations in FO with the considered effect of ICP

A schematic of the salt concentration profile across a semi-permeable membrane operating in FO mode is shown in Fig. 4.

The water flux, J_w, across the active layer is given by [8]:

$$J_w = A\,(\Delta\pi_m) \tag{11}$$

When σ in equation 6 is assumed equal to 1 (indicating the use of tight salt rejecting membranes) and $\Delta\pi_m = (\pi_{Dm} - \pi_{Fm})$ is the effective osmotic pressure difference across the active layer, then

$$J_w = A(\pi_{Dm} - \pi_{Fm}) \tag{12}$$

The reverse salt flux, J_s, across active layer is expressed by:

$$J_s = B\ (C_{Dm} - C_{Fm}) \tag{13}$$

where B is the solute permeability coefficient of the membrane. Water permeation across the membrane tends to dilute the draw solution in the supportive layer, i.e. reduce the concentration by water convective flow through the membrane. This is balanced by dilutive ICP to restore the concentration balance by creating diffusion flow of solutes from draw solution to the membrane surface. Thus, the salt flux across the porous support is the sum of the diffusive component, driven by the salt concentration gradient, and the convective component, arising from the permeation of water through the membrane,

$$-J_s = -D_s \frac{dC(x)}{dx} + J_w C(x) \tag{14}$$

where D_s is the effective diffusion coefficient of the draw solute in the porous support layer. The latter can be related to the bulk diffusion coefficient, D, by accounting for the porosity, ε, and tortuosity, τ, of the support layer, $D_s = \frac{D\varepsilon}{\tau}$.

At a steady-state, the salt fluxes across the active layer, (Eq. 13), and support layer, (Eq. 14), are equal:

$$\frac{dC(x)}{dx} - \frac{J_w}{D_s} C(x) = \frac{B}{D_s}(C_{Dm} - C_{Fm}) \tag{15}$$

Integrating Eq. (15) across the support layer thickness, from the porous layer draw solution interface, $x = 0$, where the salt concentration is C_{Ds} to the porous active layer interface, $x = -t_s$, where the salt concentration is C_{Dm} (Fig. 4(a)), yields:

$$C_{Dm} = C_{DS} \exp\left(-J_w \frac{S}{D_s}\right) + \frac{B}{J_w}\ (C_{Dm} - C_{Fm})\ \left[\exp\left(\frac{-J_w S}{D_s}\right) - 1\right] \tag{16}$$

where $S = t_s\tau/\varepsilon$ is the support layer structural parameter. The tortuosity factor τ is an overall index of the intricate pore structure. It is related to pore geometry that involves pore cross-section irregularities and a pore length parameter. Pore tortuosity can be seen as dependent upon the frequency of pore diameter variation per unit length of the characteristic particle dimension. The tortuosity factor, τ, lumps together the pore length and pore cross-section variation effects. For accurate work, τ must be determined experimentally. More information about the physical meaning of tortuosity is given by [9].

The term S/D is called the solute resistivity and is a measure of salt transport in the membrane support layer. It is used to measure the solute's ability to diffuse into or out of the membrane support layer, and it can reflect the degree of ICP in the support layer. Smaller S/D values mean less ICP, resulting in higher pure water flux J_w. One may define K (= S/D) as:

$$K = (t \cdot \tau)/(\varepsilon \cdot D_s) = \frac{S}{D_s} \tag{17}$$

The structural parameter S determines the ICP in the membrane support layer. Therefore, in newly developed membrane, it is necessary to characterize the membrane structural parameter S. The subject of ICP is discussed further in [10].

Eq. (16) indicates that the salt concentration at the active-support interface, C_{Dm}, is the sum of two terms. The effect of dilutive ICP is described by the first term on the right-hand side. The second term accounts for the decrease in salt concentration at the membrane interface due to the reverse permeation of draw solution salt into the active layer.

As water permeates across the membrane, the feed solutes are selectively retained by the semi-permeable active layer and build up within the boundary layer at the active side, resulting in concentrative ECP. Similar to ICP, the salt flux within this ECP boundary layer comprises diffusive and convective components,

$$-J_s = -D \frac{dC(z)}{dz} + J_w C(z) \tag{18}$$

At steady-state, the salt flux within the ECP boundary layer is equal to the salt flux across the active layer (Eq. 13). Integrating the resulting equation across the ECP boundary layer from the active layer, $z = 0$, where the salt concentration is C_{Fm}, to the bulk draw solution, $z = -\delta$, where the salt concentration is $C_{F,b}$, yields

$$C_{Fm} = C_{FB} \exp\frac{J_w}{k} - \frac{B}{J_w}(C_{Dm} - C_{Fm})\left[1 - \exp\left(\frac{J_w}{k}\right)\right] \tag{19}$$

where $k = D/\delta$ is the boundary-layer mass transfer coefficient. Equation 19 reveals that $C_{F,m}$ is dependent on two terms. The first term describes the bulk feed concentration, $C_{F,B}$, corrected for concentrative ECP by the factor $\exp(J_w/k)$, while the second term represents the increase in salt concentration due to draw solute leakage across the active layer. Both $C_{D,m}$ and $C_{F,m}$ are local interfacial concentrations on either side of the active layer interface and therefore are not experimentally accessible. To circumvent this, we subtract Eq. (16) from Eq. (19) and rearrange to obtain:

$$C_{Dm} - C_{Fm} = \frac{C_{Ds}\exp\left(-J_w\frac{S}{D_s}\right) - C_{FB}\exp\left(\frac{J_w}{k}\right)}{1 + \left(\frac{B}{J_w}\right)\left[\exp\left(\frac{J_w}{k}\right) - \exp\left(-J_w\frac{S}{D_s}\right)\right]} \tag{20}$$

The osmotic pressure can be assumed to be linearly proportional to the salt concentration, meaning that the Van't Hoff equation is applicable. Hence, the effective osmotic driving force, $\Delta\pi_m$, is proportional to $\Delta C_m = C_{D,m} - C_{F,m}$.

In the analysis, the ECP in the draw solution is assumed negligible because the support layer thickness is relatively large, thereby dominating CP, i.e. $\pi_{DS} \cong \pi_{DB}$. Substituting $\Delta\pi_m$ into Eq. (12) yields an expression for the water flux in FO:

$$J_w = A\left\{\frac{\pi_{DB}\ \exp\left(-J_w\frac{S}{D_s}\right) - \pi_{FB}\ \exp\left(\frac{J_w}{k}\right)}{1 + \left(\frac{B}{J_w}\right)\left[\exp\left(\frac{J_w}{k}\right) - \exp\left(-J_w\frac{S}{D_s}\right)\right]}\right\} \tag{21}$$

Substituting ΔC_m into Eq. (13) yields an expression for the reverse salt flux in FO:

$$J_s = B\left\{\frac{C_{DB}\ \exp\left(-J_w\frac{S}{D_s}\right) - C_{FB}\ \exp\left(\frac{J_w}{k}\right)}{1 + \left(\frac{B}{J_w}\right)\left[\exp\left(\frac{J_w}{k}\right) - \exp\left(-J_w\frac{S}{D_s}\right)\right]}\right\} \tag{22}$$

These equations utilize experimentally accessible parameters and incorporate the performance-limiting phenomena of ICP and ECP as well as salt leakage across the membrane.

A similar analysis was conducted by Loeb et al. [11]. When the draw solution is placed against the membrane support layer (i.e. FO mode), dilutive ICP dominates the water flux J_w and it can be expressed by [8], as:

$$J_w = \frac{1}{K}\ln\frac{A\pi_D + B}{A\pi_F + B + J_w} \tag{23}$$

In the alternative membrane orientation (i.e. PRO mode), the effect of concentrative ICP on the water flux can be expressed by [9], as:

$$J_w = \frac{1}{K}\ln\frac{A\pi_D + B - J_w}{A\pi_F + B} \tag{24}$$

Note that the structural parameter S is an important intrinsic parameter of a membrane because it determines the ICP in the membrane support layer by membrane thickness, tortuosity, and porosity. Therefore, for a newly developed membrane, it is necessary to characterize the membrane structural parameter S. The combination of ECP and ICP reduces the osmotic pressure from $\Delta\pi_m$ to $\Delta\pi_{eff}$, and may induce membrane scaling and fouling, both of which impact water flux.

3. FO and PRO

The main differences between the FO and PRO processes are:

- In FO mode, the feed solution is in contact with the active layer of the asymmetric membrane as shown in Fig. 4, and the draw solution is in contact with the supportive layer.
- In PRO mode, the draw solution flows against the selective layer while the feed solution flows against the support layer. Both modes are shown in Fig. 7.
- The PRO process can be viewed as an intermediate process between FO and RO, where hydraulic pressure is applied in the opposite direction of the osmotic pressure gradient (similar to RO), i.e. $J_w = A\ (\sigma\pi - P)$.

However, the net water flux is still in the direction of the concentrated draw solution (similar to FO). As a result, for $\Delta p = 0$, the expressions for J_w were given above (Eq. 3). When ΔP is considered, the expression for J_w given in Eq. (23) can be extended to include the effect of the applied pressure P in the PRO mode as derived by [7],

$$J_w = \frac{1}{K}\ln\frac{A\pi_D + B\left(\frac{AP}{J_w} + 1\right)}{A\pi_F + J_w + AP + B\left(\frac{AP}{J_w} + 1\right)} \tag{25}$$

$$J_w = \frac{1}{K}\ln\frac{(A\pi_D - AP - J_w) + B\left(\frac{AP}{J_w} + 1\right)}{A\pi_F + B\left(\frac{AP}{J_w} + 1\right)} \tag{26}$$

where Eq. (25) is for PRO, active layer facing feed water, and Eq. (26) is for PRO, active layer facing draw solution.

It is noticeable here that both concentrative ECP and dilutive ECP may exist in an FO process depending on the membrane orientation. Concentrative ECP occurs in the FO mode, while dilutive ECP occurs in the PRO mode. It is notable that the effect of ECP on permeate flux can be alleviated by increasing flow turbulence. Unlike ECP, the ICP takes place within the porous support layer. It is the most troublesome phenomenon in FO processes because it cannot be easily eliminated. Therefore, the decline in water flux in FO is primarily caused by ICP and the percentage of flux reduction can be as high as 80% [12].

4. Draw solution and its solutes

The choice of suitable draw solution solutes is essential for successful FO process. The selected draw solution should have osmotic pressure higher than the feed solution. The osmotic pressures of several solutions being considered for use as draw solutions are presented in Fig. 8 [1].

The draw solution, in most FO processes, has to be reconcentrated after being diluted by water permeated through the FO membranes with an available easy and economic reconcentration process. In addition, the draw solute should exhibit minimized ICP in the FO processes. The ICP could be minimized by using draw agents of high diffusion coefficients, low viscosities, and small ion/molecule sizes; these give better permeate fluxes [6]. Other factors such as low cost, low reverse solute permeability, zero toxicity, and protection of the membrane, good bio fouling resistance, inertness, and stability at or near neutral pH should be carefully considered when selecting the draw solute/solution.

The main commercially available compounds for draw agent are mainly: volatile compounds, nutrient compounds, and inorganic salts. The major advantage of using volatile gases as draw solutes in FO is that the diluted draw solution can be separated or recovered by heating/or distillation. Nutrients (or sugars) were also used as draw solutes, and in some applications, there is no need to separate the diluted nutrient solutions further, or the diluted solutions can be reconcentrated under low pressures using loose RO membranes.

A number of researchers reviewed the progress of draw solution choices [6,12,13]. Ge et al. [12], presented Tables 1 and 2 that give an overview of the development and recovery approaches of draw solutes

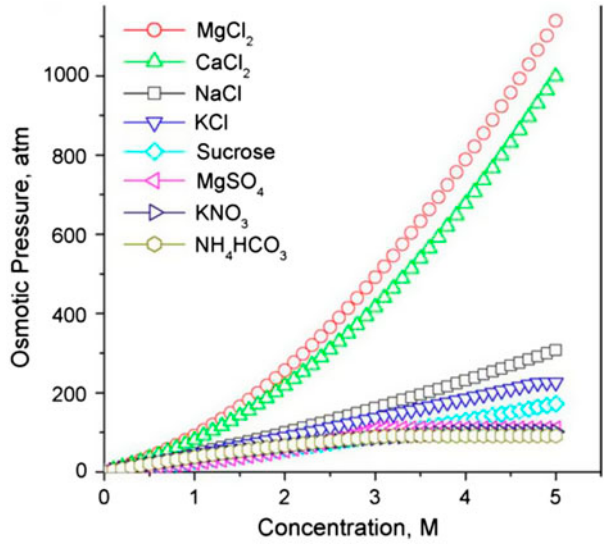

Fig. 8. Osmotic pressure as a function of solution concentration at 25°C for various potential draw solutions, data was calculated using OLI Stream Analyzer 2.0 [1].

used in FO process, and Table 2 gives the physicochemical properties and FO water flux of draw solutes used in FO processes.

The use of volatile compounds started in 1964 by Neff [14]. He proposed the mixture of ammonia and carbon dioxide gases as draw solutes for SW desalination. He outlined the details of preparing ammonium bicarbonate (NH_4HCO_3) solution from ammonia and carbon dioxide, separation of water, and regeneration of NH_4HCO_3 as well as potential applications such as irrigation, sugar, and drug concentration.

Although the use of NH_4HCO_3 as draw solute is feasible, its produced osmotic pressure is limited due to its comparatively low solubility in water. This problem was overcome by [15] and [16], who investigated mixing of ammonium salts such as ammonium hydroxide (NH_4OH) and NH_4HCO_3 at proper proportions or varying the ratio of NH_3 to CO_2 to improve the solubility. The new draw solution for FO desalination has water-soluble mixture of NH_3 and CO_2 containing (NH_4HCO_3). It can provide high water fluxes because of the high driving forces caused by the solutes high solubility. The draw solute can be recovered and decomposed to ammonia and carbon dioxide upon heating at 65°C, which were then separated from product water [17]. In principle, using small molecules, salts, and electrolytes, may not be economical and practical because of the difficulties of recovery and salt leakage. In addition, small molecule salts and electrolytes induce higher clogging in the supporting layer resulting in severe fouling and ICP. The high

Table 1
Overview of the development and recovery approaches of draw solutes used in FO technology [12]

Year	Researcher (s)	Draw solute (s)	Method of recovery	Drawbacks	Ref.*
1964	Neff	Ammonia and carbon dioxide	Heating	Energy intensive	[83]
1965	Batchelder	Volatile solutes (e.g. SO_2)	Heating or air stripping	Energy intensive, toxic	[84]
1965	Glew	Mixture of H_2O and another gas (SO_2) or liquid (aliphatic alcohols)	Distillation	Energy intensive	[85]
1970	Hough	Organic acid and inorganic salts	Temperature variation or chemical reaction	Complicated procedures, many corrosive chemical involvement	[96]
1972	Frank	Al_2SO_4	Precipitation by doping $Ca(OH)_2$	Toxic by-products	[971
1975	Kravath and Davis	Glucose	None	Not pure water	[89]
1976	Kessler and Moody	Glucose–Fructose	None	Not pure water	[90]
1989	Stache	Fructose	None	Not pure water	[91]
1992	Yaeli	Glucose	Low pressure RO	Energy intensive	[93]
1997	Loeb et al.	$MgCl_2$	None	Not pure water	[60]
2002	McGinnis	KNO_3 & SO_2	SO_2 was recycled through standard means	Energy intensive, toxic	[87]
2005–2007	McCutcheon et al.	NH_3 & CO_2 (NH_4HCO_3) or NH_4OH–NH_4HCO_3	Moderate heating (≅60˚C)	High reverse draw solute flux insufficient removal of ammonia	[40,80,84]
2007	Adham et al.	Magnetic nanoparticles	Captured by a canister separator	Poor performance, agglomeration	[106]
2007	Adham et al.	Dendrimers	Adjusting pH or UF	Not feasible	[106]
2007	Adham et al.	Albumin	Denatured and solidified by heating	Not feasible	[106]
2008	McCormick et al.	Salt, ethanol	Pervaporation-based separations	High reverse draw solute flux and low water flux	[103]
2010	Yen et al.	2-Methylimidazole-based solutes	Membrane Distillation (MD)	Materials costly	[46]
2010–2011	Ling et al. Ge et al.	Magnetic nanoparticles	Recycled by external magnetic field	Agglomeration	[42,44]
2011	Li et al.	Stimuli-responsive polymer hydrogels	Deswelling of the polymer hydrogels	Energy intensive, Poor water flux	[47,81]
2011	Ling & Chung	Hydrophilic nanoparticles	UF	Poor water flux	[79]
2011	Phuntsho et al.	Fertilizers	None	Only applicable in agriculture	[49]
2011	Iyer and Linda	Fatty acid–polyethylene glycol	Thermal method	Poor water flux	[51]
2012	Su et al.	Sucrose	NF	Relatively low water flux	[89]
2012	Ge et al.	Polyelectrolytes	UF	Relatively high viscosity	[45]
2012	Noh et al.	Thermo-sensitive solute (Derivatives of Acyl-TAEA)	Not studied	Poor water flux	[48]
2012	Yong et al.	Urea, ethylene glycol, and glucose	Not studied	Low water flux and high draw solute flux	[73]
2012	Bowden et al.	Organic salts	RO	Low water flux, energy intensive	[105]

(*Continued*)

Table 1 (*Continued*)

Year	Researcher (s)	Draw solute (s)	Method of recovery	Drawbacks	Ref.*
2012	Carmignani et al.	Polyglycol copolymers	NF	High viscosity, severe ICP	[52]
2012	Stone et al.	Hexavalent phosphazene salts	Not studied	Not economical and practical	[50]

*Ref. numbers given in this table are related and can be obtained from Ref. [12].

Table 2
Overview of the physicochemical properties and FO water flux of draw solutes used in FO processes [12]

Draw solute(s)	Conc.	Osmotic pressure (atm)	Molecular weight	Feed solution	Water flux (LMH)	Remark	Ref.*
NaCI	0.60 M	28	58.5 g/mol	DI water	9.6	CIA flat-sheet membrane, FO	[71]
$MgCl_2$	0.36 M	28	95 g/mol	DI water	8.4	CIA flat-sheet membrane, FO mode	[71]
KOH	2 M	89.3	74.6 g/mol	DI water	22.6	GA flat-sheet membrane, FO mode	[49]
NH_4HCO_3	0.67 M	28	79 g/mol	DI water	7.3	CIA flat-sheet membrane, FO mode	[71]
Sucrose	1 M	26.7	342.3 g/mol	DI water	12.9	CA hollow fiber, FO mode	[89]
PAA-Na 1,200	0.72 g/ml	44	1,200 Da	DI water	22	CA hollow fiber, PRO mode	[45]
PEG-$(COOH)_2$-MNPs 250	0.065 M	73	None	DI water	13	GA flat-sheet membrane, PRO mode	[44]
1,2,3-Trimethylimidazolium iodide	1 M	50	238 g/mol	DI water	13	CIA flat-sheet membrane, PRO mode	[46]
Sodium formate	0.68 M	28	68 g/mol	DI water	9.4	CIA flat-sheet membrane, FO mode	[105]
Polyglycol copolymer	30–70%	40–95	> 500 Da	3.5% NaCl	≥4	GA flat-sheet membrane, FO mode	[52]
Sodium hexa-carboxylatophenoxy phosphazene	0.067 M	None	1,089 g/mol	DI water	6	CIA flat-sheet membrane, FO mode	[50]

*Ref. numbers given in this table are related and can be obtained from Ref. [12].

reverse flux of NH_4HCO_3 is a serious problem [18]. The draw solute leakage not only reduces the driving force across the membrane, but also contaminates the feed product and increases the replenishment cost. Meanwhile, insufficient removal of ammonia in product water remains a big obstacle toward its complete acceptance [12].

In 1965, sulfur dioxide (SO_2) as a volatile draw solute was used by Batchelder [19]. In this work, SO_2 was added to SW or fresh water and the resultant solution was used as a draw solution in an FO process to extract water from SW. Separation of SO_2 from water was carried out by heating or air stripping.

The use of volatile compounds as draw solutes was further developed by Glew [20]. In this study, a mixture of water and SO_2 or liquid (e.g. aliphatic alcohols) was employed as a draw solution in the FO process. The purpose of adding SO_2 or alcohol was to lower the water activity and to increase the osmotic pressure of the resultant aqueous solution. Production of water and the recovery of SO_2 were proposed by means of distillation.

In 2002, a combination of potassium nitrate (KNO_3) and SO_2 were used as draw solutions by McGinnis [21] in a system consisting of two FO units for SW desalination. Hot SW and saturated KNO_3 solution were used as the respective feed and draw solutions in the first FO unit. With water permeating to the draw solution from the feed SW, the KNO_3 solution was diluted. The diluted KNO_3 solution was reconcentrated by a saturated SO_2 solution in the second FO unit. The SO_2 solute was then removed by standard means, such as heating. In this way, both KNO_3 and SO_2 were recycled.

It is noted here that the SO_2 has special physicochemical properties. SO_2 is volatile and corrosive, and its solution is acidic and unstable. It is a redox agent. It is susceptible to react with both oxidant and reducing agents. Hence, careful operations are needed for the SO_2-involved FO process and the subsequent post-treatment.

In summary, volatile draw solutes can be separated from product water by means of heating or distillation, and the regeneration of draw solutions can be achieved by dissolving the volatile gases back into water. However, most early patents on volatile compounds as draw solutes had insufficient experimental data to demonstrate their superiority or advantages.

The nutrient compounds, was proposed originally for an emergency water supply in lifeboats, but later extended to food and wine concentrations, and wastewater recycles by Herron et al. [22] and Su et al. [23]. Glucose was first explored as a draw solute in the FO process for SW desalination by Kravath and Davis [24]. Glucose present in the final product is edible and intended for drinking purpose in emergency lifeboats. Therefore, it excluded the need of draw solute recovery.

Kessler and Moody [25], investigated the use of glucose and fructose combination as draw solutes. It was claimed that better FO performance was achieved when compared with pure glucose solution. Stache [26] in 1989 refined the idea by using fructose alone as the draw solute because fructose has the merit of a higher efficiency in osmosis. In addition, there is no thirst induced after drinking, making fructose more attractive as a draw solute. Yaeli [27], extended Kravath and Davis [24] work by including glucose regeneration through a low pressure RO processes. He was the pioneer in introducing the concept of a "hybrid" system consisting of an FO and a low pressure RO. Sucrose was used as a draw solute by Su et al. [23] in wastewater treatment using double-skinned hollow fiber membranes. Fig. 9 reported by Barbera [28] gives the osmotic pressure of the glucose and sucrose solutions.

Various inorganic salts have been used in the FO process. Draw solutions formed by inorganic salts give reasonably high fluxes and can be readily recovered by RO as given by Achilli et al. [18], by Yong et al. [29] as well as Yangali–Quintanilla [30]. In 1972, a draw solution made of aqueous aluminum sulfate was developed by Frank [29] as an osmotic agent and certain salts were added to the solution to facilitate separation of salts via precipitation, as well as to neutralize the solution. A perceptible salt, aluminum sulfate ($Al_2(SO_4)_3$), was also explored as a draw solute for FO by Frank [29]. This salt could then be treated with calcium hydroxide ($Ca(OH)_2$). The resultant precipitates of calcium sulfate ($CaSO_4$) and aluminum hydroxide ($Al(OH)_3$) were removed from the product water. Subsequently, H_2SO_4 was added to neutralize the excess $Ca(OH)_2$ left in the water. The drawbacks of afore-mentioned two approaches are obvious in view of the complicated post-treatment procedures and the involvement of many chemicals including both base ($Ca(OH)_2$ and $Al(OH)_3$) and acid (H_2SO_4).

The concentrated brine of the last stage in MSF/MED is suggested as a draw solution by Alatee et al. [31], and Mabrouk [32]. In this case, there is no need for recovery methods and no addition in cost. The diluted brine is fed back to the MSF or MED as a feed. This increases the top brine temperature (TBT) in MSF up to 135˚C, and up to 85˚C in MED [30,33].

5. FO membranes

Lack of commercial FO membranes hinders broad advancement of FO application. Ideal FO membranes should have: high density of the active layer for high solute rejection, thin membrane support layer with minimum porosity for low ICP, and therefore, higher

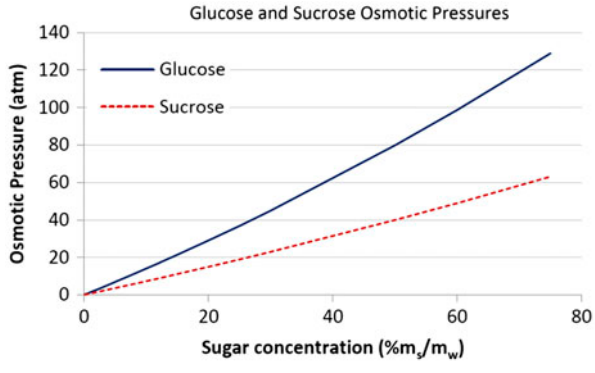

Fig. 9. Osmotic pressure of glucose and sucrose as a function of concentration. Values calculated using OLI's software [28].

water flux (low transport resistance) to minimize IPC, hydrophilicity for enhanced flux and reduced membrane fouling, and high mechanical strength to sustain hydraulic pressure when used for PRO. Studies on water transport through FO membranes show that ICP within the support layer significantly reduces membrane flux, e.g. Gray et al. [9], Coday [34] and McCutcheon and Elimelech [3,38].

Initially, RO membranes were employed for FO processes, but recently FO membranes have been designed and manufactured. The thickness and transport resistance of the support layer plays a critical role in FO membrane performance, in contrary to the RO and nanofiltration (NF) membranes. Most of commercially available RO semi-permeable membranes, such as the widely used polyamide thin-film membranes, have a very thick woven fabric support that would restrict their application as FO membranes. The thickness of successful and commercially available FO membrane support layers, as reported by Saren et al. [31], is between 40 and 90 μm for woven fabric supported membranes. This is much thinner than that of conventional thin film composite (TFC) RO membranes (~150 μm).

The first generation of FO membranes using cellulose triacetate chemistry was produced by hydration technology innovations (HTI), as reported by Coday [32]. This polymer is cast with an embedded polyester mesh for membrane support, while forming a thin, dense semi-permeable active layer [1] and [32]. HTI's goal was to minimize the thickness of the asymmetric membrane active layer, increasing water permeability without compromising contaminant rejection or membrane integrity. These first generation membranes have relatively low water permeability and salt rejection and they can only operate in a narrow pH range, as reported by Qiu et al. [35] and Wang et al. [36]. Recently, efforts have focused on the development of FO TFC membranes, as reported by Qiu et al. [35], Wang et al. [36], and Yip et al. [37] with the main goals of increasing membrane water permeability using improved casting techniques and providing greater chemical stability in a wider pH range.

The known two existing types of the FO membranes are:

(1) Cellulosic membranes realized through phase inversion, made of cellulose acetate or polybenzimidazole (PBI), and are characterized by high hydrophilicity and low fouling propensity, good mechanical strength, and resistance to chlorine and oxidants [20]; at the same time, these materials are easily susceptible to hydrolysis and biological attack. Thus, the pH must be strictly maintained in the range of 4–6 and temperature must be up to 35˚C [28].
(2) Membranes of multiple layers, known as TFC. They have an overall thickness of approximately 50 μm, and are very different from RO thin composite film membranes in that the thick polysulfone support is replaced with a polyester mesh [6].

With regard to membrane modules, both flat-sheets plate-and-frame, tubular, and hollow-fiber configurations have been developed. Spiral wound modules are not suitable for operation in FO mode because the draw solution cannot be forced to flow into the envelope formed by the membranes [1]. Until recently, both hollow fiber and flat-sheet TFC polyamide membranes have been fabricated for FO applications. In fact, most of the methods used for the preparation of these membranes are the same as those for developing TFC polyamide RO membranes: phase inversion for the preparation of a porous substrate, and then interfacial polymerization for the formation of a thin polyamide active layer.

Recently, two types of TFC FO hollow fibers with an ultra-thin polyamide-21 based on RO-like skin layer (300–600 nm) have been developed by Wang et al. [34]. The TFC layer could be fabricated on either the outer surface or inner surface of a porous hollow fiber substrate. Both membranes appeared to show excellent water fluxes and salt rejection. The membranes were found to be very hydrophilic and show very low pore size distributions. To date, the membrane with the TFC layer on the inner surface is believed to be superior to all FO and NF membranes used in FO processes which have been reported in the literature by Wang et al. [34].

Furthermore, a hollow fiber FO membrane made of PBI has been developed by Flanagan [38]. The PBI membrane can generate high flux in FO process and is thus a very promising material for FO membrane development, even though the salt rejection of this membrane in the current stage is relatively low.

Zhao et al. [6], showed cross-sectional SEM images of two commercially FO membranes. The first image (denoted as FO-1), Fig. 10(a) has a very thin overall thickness (~50 μm), while the second one (denoted as FO-2), Fig. 10(b) is much thicker (>100 μm). Both of them are asymmetric and thought to be made of cellulose triacetate (CTA) [1]. Most researchers use the first type of membrane in their FO studies because of its higher water flux as compared to the second type. Fig. 9(a) shows that the FO-1 membrane consists of at least three parts: a thin selective layer on one side, a relatively loose support layer on the other side, and

an embedded mesh in the middle. The FO-1 membrane is distinctively different from the conventional TFC membrane in that it is mechanically supported by an embedded polyester mesh rather than the thick support layer existing in a RO membrane. The structure of the FO-2 membrane is similar to that of the conventional TFC membrane as shown in Fig. 9(b). According to the HTI patent, the FO-2 membrane has three layers: a skin layer (8–18 μm) made from polymeric material, a porous scaffold layer (25–75 μm), and a hydrophilic support fabric. This type of FO membrane is also made of cellulose triacetate and it provides higher salt rejection, but lower water flux when compared to the FO-1 membrane.

Zhao et al. [6], presented an overview of the FO membrane developments in the last decade, and summarized in Table 3. According to their fabrication methods, these recently developed membranes can be classified into three categories: phase inversion-formed cellulosic membranes, TFC membranes, and chemically modified membranes (Fig. 10).

6. Membrane fouling

Membrane fouling is a major issue in FO operation. FO flux reduction can be strongly affected by membrane structure and orientation in addition to other operational conditions. FO fouling is generally more pronounced when the active rejection layer is facing the draw solution (AL-DS or case b in Fig. 7), since this orientation is prone to severe internal pore clogging in the porous membrane support layer [6]. The modification of the support layer structure (e.g. reduced porosity, increased tortuosity, or increased thickness in the case of a cake layer formed on the support surface) in the AL-DS orientation may further enhance the ICP in the membrane support, leading to accelerated flux reduction. Compared to the AL-DS orientation, the active-layer-facing-feed-solution orientation (AL-FS or case a in Fig. 7) generally enjoys more stable flux performance, although its more severe ICP level means that this membrane orientation tends to have relatively lower water flux. Thus, one may operate an FO membrane either (1) in AL-DS to attain a significantly higher initial flux (but with much higher fouling propensity) or (2) in AL-FS to achieve an inherently more stable flux at the expense of more severe ICP. Correspondingly, it is anticipated that different membrane operation and fouling control strategies may be adopted depending on the membrane orientation. Furthermore, membrane fouling in FO and RO has been compared and is thought to be quite different from one another in terms of the reversibility and water cleaning efficiency [6]. It is observed that membrane fouling in FO is almost completely reversible while it is irreversible in RO.

However, they attributed FO fouling to the accelerated cake-enhanced osmotic pressure (CEOP) due to reverse salt diffusion from the draw solution. Recently, it was reported that silica scaling of FO membranes, resulting from the polymerization of dissolved silica, was the dominant inorganic fouling in real SW desalination. Silica polymerization could also accelerate organic fouling, which is much more easily removed by water rinsing as compared to silica scaling [39].

7. FO arrangements in desalination

An example of how to use the FO process in desalting SW is illustrated in Fig. 11. The SW (as a feed) and draw solution of an osmotic agent are circulated on opposite sides of the FO membrane. Water flows out of the feed SW through the FO membrane to dilute the osmotic agent, while SW is concentrated. The osmotic agent is reconcentrated in an evaporator and recirculated. It is clear that the process of evaporating the draw solution to get the product is energy intensive and expensive. The evaporator should be replaced with a different, less energy comprehensive, unit.

A crystallizer can be used in the case of an osmotic agent whose solubility could be manipulated through temperature or pH, or an air stripper can be used if a highly volatile agent was identified [3]. This secondary process to be used to reconcentrate the draw solution, producing water with substantially less TDS compared to the feed, should consume energy or fuel resource less than those of conventional alternatives such as RO system or evaporation method. The fouling and scaling phenomena in the FO membrane system may be substantially reduced than that of the RO.

McCutcheon et al. [15], suggested a novel FO desalination process shown in Fig. 12. The feed to the FO unit is SW, and the draw solution is NH_4HCO_3 composed of two highly soluble gases: ammonia (NH_3) and carbon dioxide (CO_2). The concentrated draw solution is made by dissolving NH_4HCO_3 salt in water. Spiral wound or hollow fiber semi-permeable membrane modules were suggested for the FO unit. Water flows from SW across the membrane to the NH_4HCO_3 draw solution. The diluted draw solution is sent to a separation unit, consisting of distillation column or membrane gas separation unit to yield potable water, see Fig. 12.

Table 3
Recent FO membrane developments [6]

Year	Membranes	Materials	Preparation methods
2005	Capsule wall membrane	Cellulose acetate or ethyl cellulose	Dip-coating, phase inversion
2007	Hollow fiber NF	Polybenzimidazole (PBI)	Dry-jet wet phase inversion
2008	Flat-sheet cellulose acetate membrane	Cellulose acetate	Phase inversion and then annealing at 80–95°C
2009	Dual-layer hollow fiber NF	PBI-PES/PVP	Dry-jet wet phase inversion (i.e. coextrusion technology)
2010	Hollow fiber	PES substrates, polyamide active layer	Dry-jet wet spinning and interfacial polymerization (IP)
2010	Hollow fiber NF	Cellulose acetate	Dry-jet wet spinning
2010	Flat-sheet double-skinned	Cellulose acetate	Phase inversion, and then annealing at 85°C
2010	Flat-sheet TFC membrane	Polysulfone (PSf) support, Polyamide active layer	Phase inversion and IP
2010	Double dense-layer membrane	Cellulose acetate	Phase inversion
2011	Modified RO	PSf support modified by polydopamine	Chemical coating
2011	Flat-sheet composite	Cellulose acetate cast on a nylon fabric	Phase inversion
2011	Flat-sheet composite	PAN substrate, multiple PAH/PSS polyelectrolyte layers	Layer-by-layer assembly
2011	Positively charged hollow fiber	PAI substrate treated by PEI	Chemical modification
2011	Positively charged flat-sheet	PAI substrate treated by PEI	Chemical modification
2011	Flat-sheet TFC polyamide	PES/SPSf substrate, Polyamide active layer	Phase inversion and IP
2011	Flat-sheet TFC polyamide	PES/sulfonated polymer substrate, Polyamide active layer	Phase inversion and IP
2011	Flat-sheet TFC	PSf support, polyamide active layer	Phase inversion and IP
2011	Nanoporous PES	PES cast on PET fabric	Phase inversion
2011	Cellulose ester membrane	Cellulose ester	Phase inversion
2011	Flat-sheet TFC polyamide	PES nanofiber support, polyamide active layer	Electrospinning and IP
2011	Flat-sheet TFC polyamide	PSf nanofiber support, polyamide active layer	Electrospinning and IP

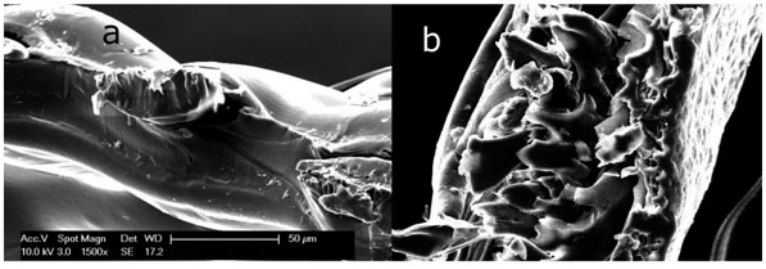

Fig. 10. The cross-sectional SEM images of FO membranes from HTI: (a) FO-1; (b) FO-2. The SEM images taken in Adelaide Microscopy [6].

The NH_3 and CO_2 are separated from the draw solution and recycled back to the FO unit. Because of the relatively low temperature heat requirements of NH_3 and CO_2 removal, the separation stage can utilize low-grade heat, which is a common byproduct of electricity production. The high solubility of the

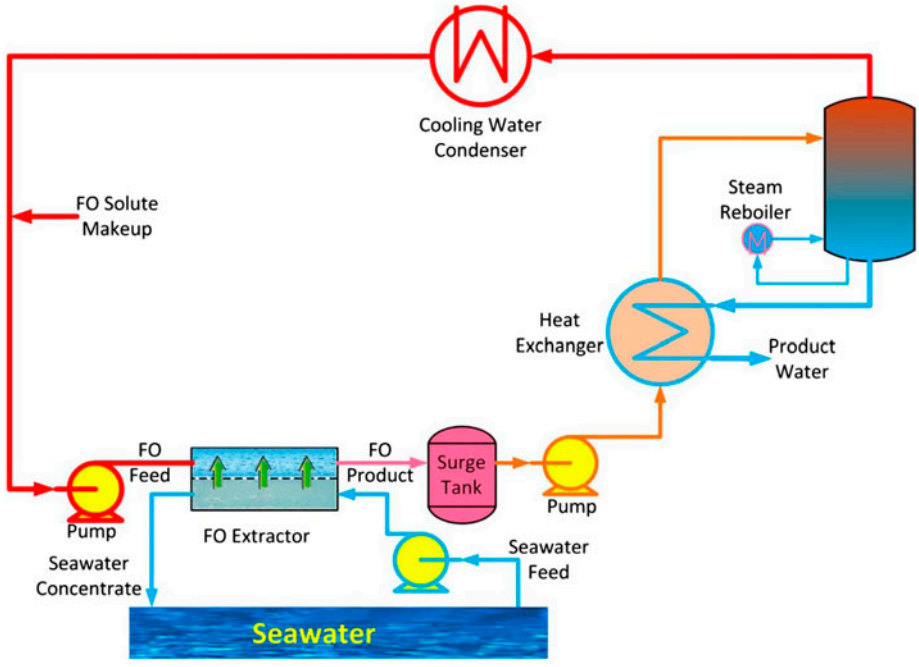

Fig. 11. Forward osmosis desalination plant (FODP) process schematic, reproduced from [5].

NH_4HCO_3 salt leads to a very high osmotic efficiency. Calculated osmotic pressure as a function of draw solutes concentration is shown in Fig. 13. The calculation shows that osmotic pressures far greater than that of SW can be generated in the draw solution, providing the necessary driving forces for high potable water flux and high recovery. Upon moderate heating (near 60°C), NH_4HCO_3 can be decomposed into ammonia and carbon dioxide gases [16]. The gases are then removed from solution by low-temperature distillation using relatively low energy apparatus. Other gas separation processes, such as membrane-based technologies, can also be used.

McGinnis et al. [40], calculated energy requirements for NH_3–CO_2 solution separation with distillation columns and proposed a multistage column distillation (MSCD) technique, which utilizes the waste heat of the previous-stage column to increase thermal efficiency.

It is noticed that energy required in this approach is almost entirely thermal, with a small amount of additional electrical power used for fluid pumping to and from the column. All gases in the vapor stream from the top of the column are condensed at the vacuum level of the column, with noncondensable gases (external air from fitting leaks) removed with a steam thermal compressor.

Semiat et al. [35], presented Fig. 14 and Table 4 that account for the energy consumed by this process.

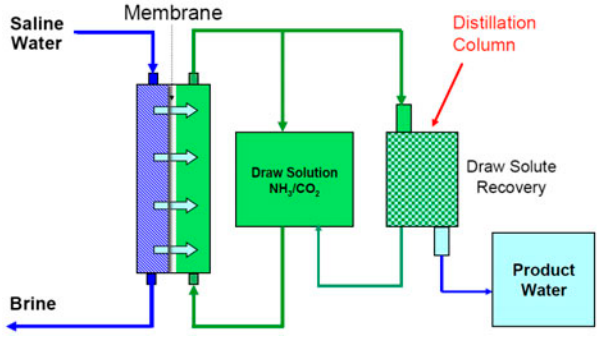

Fig. 12. Schematic diagram of FO desalting system [15].

In addition, they encountered additional costs in this process as follows:

- Heat energy is required for the separation of the ammonia and CO_2 from the solution and for the evaporation of large amounts of water.
- An additional water purification step, such as ion exchange, is required to ensure that the final product contains less than 1 ppm NH_3.
- The gas phase containing ammonia, CO_2, and water vapor is adsorbed on part of the diluted draw solution to increase its concentration; energy expenses can be reduced by performing the desorption–adsorption at a low pressure to

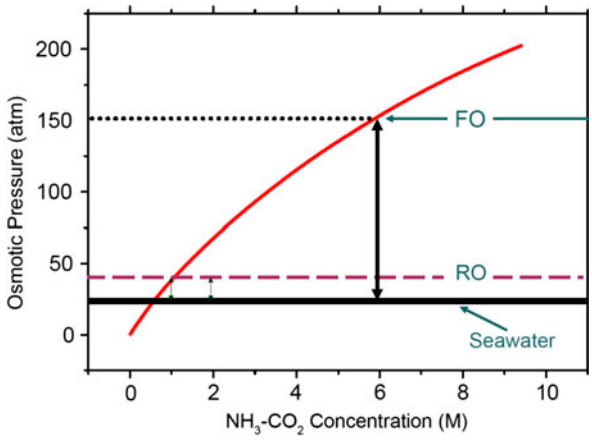

Fig. 13. Osmotic pressure generated by NH_4HCO_3 solution at 50˚C, the horizontal dashed lines represent the osmotic pressure of the feed water undergoing water recovery [17].

allow use of low-grade heat from the consumed steam. It was also assumed that product water still contains 9 ppm (ppm) of ammonia, which can be further reduced by cheaper techniques, such as ion exchange. The results shown in Table 2 indicate that the specific energy needs of the process are around 13 ± 3 kWh/m^3, about 4 times higher than energy requirements of RO SW desalination system.

Also, Danasamy [36], reported that the separation of product water and the recovery of NH_4HCO_3 draw solutions can be carried out through thermal processes. Upon moderate heating of around 60°C, NH_4HCO_3 decomposes to ammonia and carbon dioxide gases and separates from the product water. The overall energy required in the FO desalination and NH_4HCO_3 draw solution recovery has been predicted by using a chemical process modeling software (HYSYS). Both thermal and electrical energy needed were calculated when distillation columns were used to separate draw solutes from the product water. The majority of energy consumption was the thermal process for NH_4HCO_3 recovery. The heat requirement with a single distillation was more than 75 kWh/m^3. In contrast, the electrical power requirement of a single FO process in desalination was less than 0.25 kWh/m^3. Therefore, although NH_4HCO_3 solution can produce a high osmotic pressure and result in a good water flux, its recovery is still an energy-intensive process. Unless sources of waste heat are available at low costs, the NH_4HCO_3-based SW desalination may not be practical. In addition, a significant ICP phenomenon has been observed which leads to a significant water flux decline. Furthermore, the quality of product water may not meet the drinking water standard when real SW is used as the feed solution because of the presence of nonvolatile organic species from NH_4HCO_3 and higher boron concentration in the FO permeate.

Development of energy-efficient draw solution recovery processes is a promising area, but these processes are still not sufficiently well established to be implemented in real systems. Kim et al. [37], investigated the FO processes with solution recovery to determine the feasibility and costs of an industrial-sized system when three draw solutes, namely, NH_4HCO_3, NH_4OH, and ethanol remained are used.

8. The single commercial FO desalting plant

The only FO or manipulated osmosis desalination (MOD) process on a commercial scale was reported by a company called Modern Water Plc. [41]. The FO system and solute regeneration system were integrated in single cycle as shown in Fig. 15. The basic principles of this process, in all its variations, is an initial FO step followed by a regeneration step to reconcentrate the osmotic agent/draw solution for reuse and to separate the "desalinated" water, prior to any post-treatment. This process of course can be used for "dewatering" or concentration of the feed solution. The regeneration step can be thermal-based as given before, or membrane-based. Modern Water used RO in the draw solution regeneration step, as shown in Fig. 15. Thus, this process can be considered as RO process with FO as pretreatment.

In summary, concentrated osmotic agent is used as a draw solution to draw fresh water from the feed SW in the FO system. In doing so, the osmotic agent becomes diluted. The diluted osmotic agent is then "regenerated" by the removal of this fresh water in the regeneration system, which can be RO process. The two main claimed advantages over conventional RO are lower fouling tendency and lower energy consumption.

The lower fouling potential of the FO process compared to RO system has been shown on a commercial SW plant in Oman. No chemical cleaning was required over several years of operation as claimed by Modern Water Plc. [41], while conventional SWRO required cleaning every few weeks with several membrane changes. The result is reduction in the use of membrane cleaning chemicals and improved availability.

Lee et al. [42], systematically compared the fouling behaviors in FO and RO systems. They found that the key mechanism of flux decline in FO

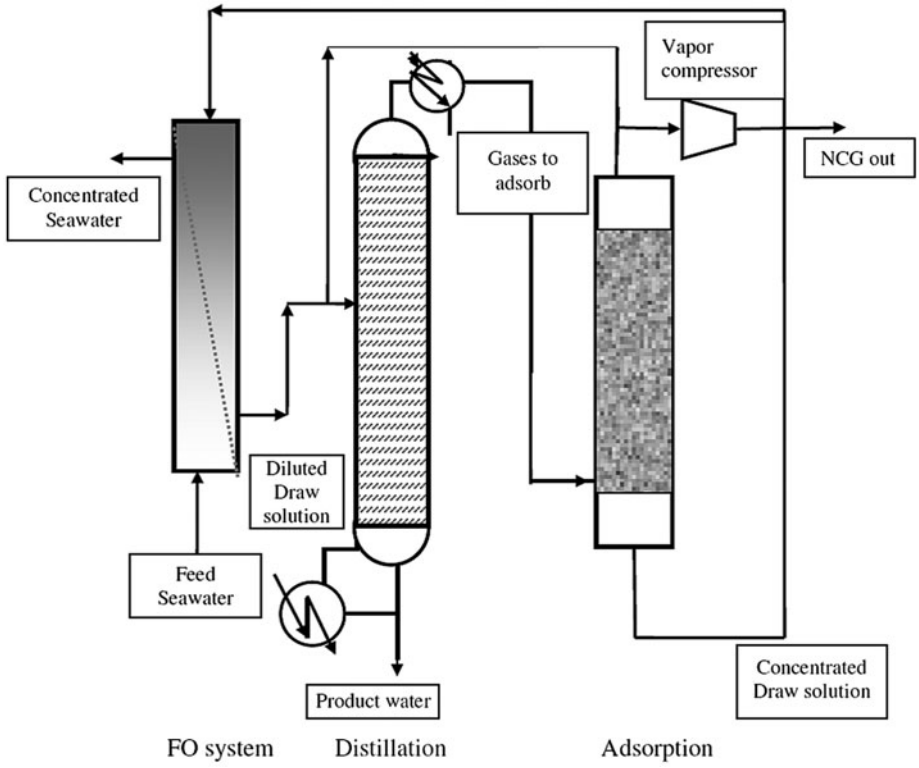

Fig. 14. Basic sections in forward desalination [35].

Table 4
Estimated energy needs in the FO process of Fig. 14.

Operation	Estimated consumed energy	Remarks
Pretreatment and concentrate disposal	1.7	Pumping, filtration, etc. similar to RO plant
Pumping water and draw solutions through the membranes	0.3	
Evaporator distillation energy consumption	3.0	Electricity charge of 13 kWh per ton of exhaust steam
Cooling water at the distillation column	3	Pumping energy requirement
Cooling water for adsorbing draw solution gases	4	Pumping energy requirement
Vacuum pump for noncondensable gases removal	4	
Credit for cooling water saved in power station for steam supplied to distillation column	−3.0	Removal of heat from 250 kg of steam
Total	13	±20% error estimate

process is rather accelerated CEOP due to reverse salt diffusion from the draw to feed than the increase in fouling layer resistance. This implies that selecting the proper draw solution (i.e. less back diffusion) and/or improving the membrane property (i.e. higher selectivity) are of paramount importance in efficient operation of FO process. Interestingly, fouling in FO process is almost reversible while irreversible in RO system. Deformable organic foulant without hydraulic pressure (i.e. FO) makes loose and sparse fouling layer that can easily be removed by simple physical cleaning. Fouling control and membrane cleaning in FO are much more feasible than RO since FO fouling is reversible by simple physical cleaning.

The potential for lower energy consumptions was given by an example which compares the energy consumption between [41]:

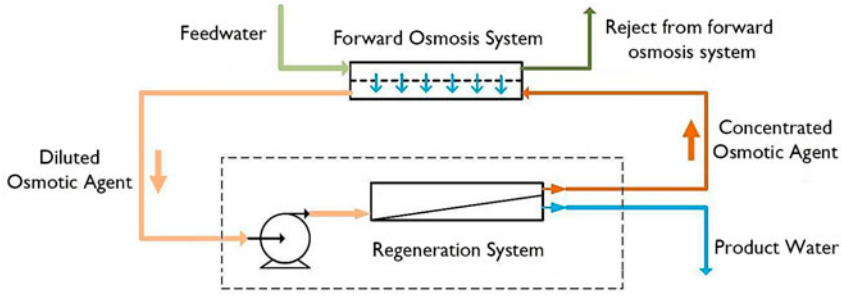

Fig. 15. Simplified manipulated osmosis process diagram [41].

- SWRO with dual media filtration (DMF) as pretreatment (SWRO/DMF).
- SWRO with DMF and ultra-filtration (UF) as pretreatment (SWRO/DMF/UF).
- SWRO with DMF and FO as pretreatment (SWRO/DMF/FO).

For typical conditions of: 1,000 m^3/d product flow, 40% overall recovery, 40% FO recovery, and 50% regeneration recovery, the total specific energy consumption in kWh/m^3 of product were 6.39 for (SWRO/DMF), and 6.24 for (SWRO/DMF/UF), and 5.89 for (SWRO/DMF/FO), respectively.

9. FO research projects at QEERI

9.1. FO and RO hybrid system

The first project idea is to co-treat SW and tertiary treated wastewater (TTWW) to produce potable quality conditions at a reduced energy consumption compared with a SWRO system. Desalted water is the main nonconventional water resource in Qatar, and its production is expected to reach 480 Mm^3/y in 2014. Treated wastewater (TWW) of the tertiary level is another water source that should be fully utilized in Qatar and all GCC. In Qatar, about one-third of municipal wastewater (WW) is now treated (≅ 354,000 m^3/d or 129.4 Mm^3/y) to the tertiary level TWW, and there is TWW project under construction of 439,000 m^3/d (or 160 Mm^3/y) to the same tertiary level TWW. Hence, total TWW of 290 Mm^3/y of TTWW would be available. Some are recycled to be used for the irrigation of few crops and landscaping, while the rest is dumped back into the gulf. Extending the treatment of TTWW of limited usage to potable water quality of unlimited usage can open the door to use TWW as part of municipal water. This improves the water security by not becoming completely dependent on the DW, and reduces the negative environmental impact.

Despite the common use of RO system for desalination and treatment of TWW worldwide, the RO membranes fouling and scaling require intensive chemical cleaning that can increase the treatment cost and decrease membrane lifetime. In addition, the use of scale inhibitors can add cost and complexity to system operation. High-energy demand for RO is another factor hindering the use of SWRO, especially in locations of high salinity, e.g. SW salinity in West Qatar's shore reaches up to 57,000 ppm, while it can reach 48,000 in the East. The SWRO consumed energy is usually reduced by using energy recovery devices (ERD).

Dilution of SW provides another method to reduce the energy demand during RO desalination of high salinity SW. The dilution decreases the osmotic pressure, which must overcome to produce the RO permeate. The relatively low salinity of TWW makes them good candidates for use in diluting saline streams before desalination. Nevertheless, direct dilution may contaminate and alter the chemistry of the feed stream to the desalination process, intensify membrane fouling, and may subsequently reduce product water quality. The use of water chemical potential of SW as the driving force to induce clean water from TWW stream to SW stream through FO semi-permeable membrane provides several benefits, which include:

- The osmotic pressure difference of high salinity SW draw solution (π_D) and feed TWW (π_F) provides the required water chemical potential difference (μ_F–μ_D) that induces the water flow from the TWW to the SW without the need of extensive pumping energy.
- Dilution of SW before RO system lowers energy consumed for desalinating the SW.
- Provides a multi-barrier protection against TWW to pass through the FO and RO membranes to produce drinking water quality.
- Reduced RO membrane fouling.

- The draw solution is a readily available renewable water source (e.g. SW), and its reconcentration is not needed.

The technical and economic feasibility of a FO and RO hybrid process to co-treat saline water, such as SW, and impaired water such as TTWW were outlined in [43]. In this hybrid process, SW is diluted to reduce its osmotic pressure and thus reduces its energy demand if desalinated by the RO desalting system. The contamination of the relatively low salinity TTWW is removed by use it as a feed stream in the FO process and its permeation through the FO membrane to dilute the SW before its desalination. In the first FO stage process, Fig. 16, the TTWW is acting as the feed stream, while the SW is acting as the draw agent stream. The driving force is the water chemical potential difference between the two streams causing water to diffuse spontaneously through the FO membrane from the TTWW into the SW stream.

In Fig. 16, the FO first stage uses SW (TDS = 45 g/l, and flow rate = 100 m^3/d) as a draw solution to extract water from feed TTWW (TDS = 1 g/l, and flow rate = 100 m^3/d). As a result, the SW is diluted from TDS = 45 to 30 g/l. This means increasing draw solution (D) flow rate from 100 m^3/d to 150 m^3/d, and reducing feed solution (F) flow rate from 100 m^3/d to 50 m^3/d. This FO stage uses the osmotic pressure differential as the driving force, drawing water through a semi-permeable membrane and rejecting almost all dissolved contaminants in the process. The diluted SW is processed through an RO desalination system, which rejects salts and dissolved contaminants that may have crossed the membrane from the feed TWW. The RO recovery rate can be increased to 55%, with brine salinity close to 67 g/l. If the feed to the RO is 150 m^3/d, and the recovery ratio is 55%, the permeate would be 82.5 m^3/d. The TWW after first stage FO with TDS=2 g/l and flow rate of 50 m^3/d used in the second stage FO as feed stream and the RO concentrated brine with TDS = 67 g/l and flow rate = 67.5 m^3/d as draw agent. The second stage FO is designed to dilute the RO brine before being dumped into the gulf. The FO membrane area will be calculated to dilute the concentrated brine to 45 g/l and flow rate of 100 m^3/d, same conditions as the SW conditions at the system intake.

The energy saving due diluting the SW from TDS = 45 g/l to 30 g/l can be determined by calculating the energy consumed by the high pressure feed pump to the RO membranes for the same permeate output. This pump consumes about 80% of the RO total energy consumption. Before dilution, TDS = 45 g/l, the recovery ratio is 35%, and the applied pressure is close to 65 bar, and permeates of 82.5 m^3/d (0.955 l/s), the consumed energy by the pump is:

$$W_p = Q_f(\mathrm{m^3/s}) \times P_f(\mathrm{kPa})/\eta_p = \left(\frac{0.955}{1,000 \times 0.35}\right) \times 6,500/0.8 = 22.17\ \mathrm{kW} \quad (27)$$

After dilution, the TDS = 30 g/l, the overall recovery ratio is 55%, and the applied pressure is 50 bar, and then the consumed energy by the pump is:

$$W_p = \left(\frac{0.955}{1,000 \times 0.55}\right) \times 5,000/0.8 = 10.85\ \mathrm{kW} \quad (28)$$

Therefore, energy consumed by the RO high pressure feed pump is decreased more than 50% after dilution. The second-stage osmotic dilution process dilutes RO brine before discharging and further concentrates and reduces the volume of the TWW stream. Thus, the energy demand of the desalination plant is decreased, and two significant barriers are in place to reject contaminants in the impaired stream. This arrangement has several advantages, which can be listed as follows:

- The dilution of SW before RO system results in lowering energy consumption of the system.
- It provides multi-barrier protection of drinking water.
- Reduces the RO membrane fouling.
- Safe and beneficial reuse of TWW.
- The draw solution is a readily available renewable source (e.g. SW) that has relatively high osmotic pressure and does not require reconcentration; the process can operate with both the feed and draw solution in a once through configuration.
- It provides the benefits of FO (e.g. low energy operation and high resistance to irreversible fouling), while simultaneously eliminating energy costs associated with draw solution reconcentration.
- A SW intake can readily supply fresh draw solution, and accumulation of sparingly soluble salts in the draw solution is not expected because the draw solution is not recycled in the process.
- The volume of the TWW is minimized.
- The second-stage FO can be used as PRO system for power generation.
- Membranes with higher water permeability (A) would make the process even more practical. Despite the low-water flux through current ODMP membranes, implementation of osmotic dilution to enhance SW RO (SWRO) desalination could be possible and economically viable.

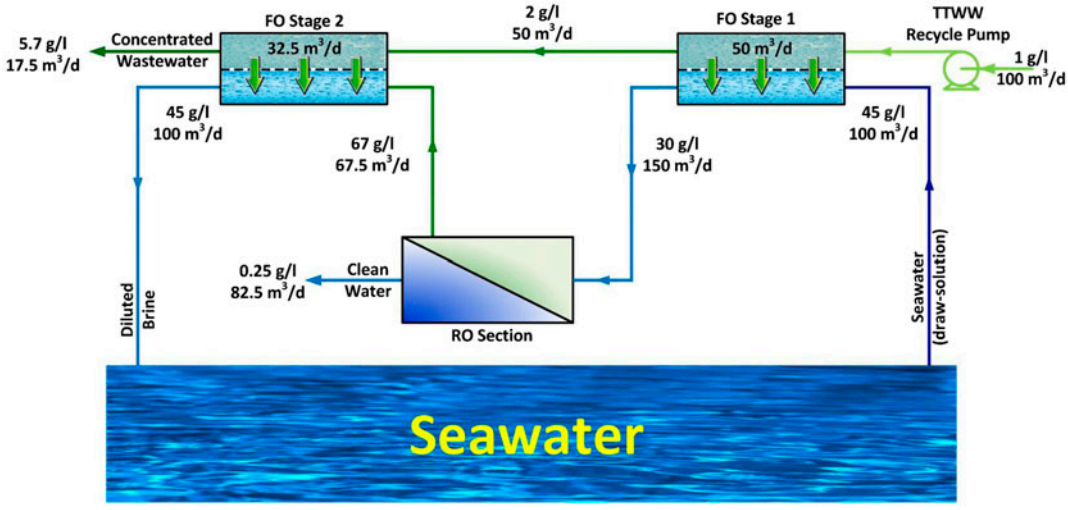

Fig. 16. Schematic drawing of a novel hybrid osmotic dilution (ODN)/SWRO process, reproduced from [43].

9.2. Feasibility of using FO as pretreatment for once-through (OT) MSF system

The second project is to study the viability of using FO as pretreatment for once-through multi stage flash (OT-MSF) desalting system. The suggested project is using FO as pretreatment for a OT-MSF to raise the TBT from the conventional 110 to 150˚C if FO is capable to remove the ions causing the $CaSO_4$ scale formation.

Fig. 17 shows the TBT which can be achieved when the feed water was fully or partially treated by nanofiltration (NF) to remove the scaling constituents. The NF process was suggested for the removal of divalent ions such as Ca^{2+}, Mg^{2+}, and SO_4^{2-} from feed water to the thermal desalination processes. Removal of Ca^{2+}, Mg^{2+}, and SO_4^{2-} would allow raising the TBT and result in increasing gain ratio (GR) of MSF. NF is a membrane process that consumes good amount of energy, and the application of using NF as pretreatment proved to be uneconomical with many technical complications. The idea of using FO as pretreatment was suggested recently for brine recirculation MSF [30,33]. However, it is suggested here for OT-MSF, Fig. 18. Moreover, the concept of using FO for pretreatment was never proved experimentally. The suggested arrangement is shown in Figs. 19 and 20. It is much easier to apply this pretreatment on OT-MSF unit compared to brine recirculation one. The process calculations showed that for the same performance ratio, the heat transfer area of once-through long tube (MSF-OT-LT) MSF is 34% lower than that of brine recycle MSF-BR evaporator. This is due to the flashing range increase and higher heat transfer coefficient of MSF-OT-LT configuration. The pumping power of the MSF-OT-LT is 40% lower than that of MSF-BR-CT evaporator. This is due to lower friction loss in the tubes and due to the removal of the brine recycle pump [33]. This study showed that the MSF-OT-LT evaporator is a viable option for large-scale capacity and a reliable technology for poor quality and high salinity SW [33].

The FO process operates at atmospheric pressure with a semi-permeable membrane separating the incoming SW, acting as feed stream, and the concentrated brine, acting as the draw agent. The SW feed solution contains 42 g/l total dissolved solids (TDS), and the draw solution of TDS = 73.3 g/l. Fig. 18 shows the SW inlet flow rate as 30 m^3/h of TDS = 42 g/l, and leaving as 20 m^3/h at TDS = 63 g/l, with 10 m^3/h permeated to the brine (B) side through the FO membrane. The brine inlet to the FO unit as draw solution with flow rate 45 m^3/h at TDS = 73.3 g/l, and leaving as 55 m^3/h at TDS = 60 mg/l. Thus, the permeate is 10 m^3/h from the SW side to the B under the potential of osmosis pressure difference ($\Delta\pi$). Average salinity at the feed SW side 52.5 g/l with average osmotic pressure of 40.425 bar. Average salinity at the brine side is 66.5 g/l with average osmotic pressure of 51.05 bar. This gives osmotic pressure differential ($\Delta\pi$) equal to 10.78 bar.

9.2.1. FO and OT-MSF system analysis

The brine (draw solution) flow from the FO unit at 55 m^3/h and 60 g/l is the feed to the OT-MSF operating at TBT up to 150°C. The temperature of the last

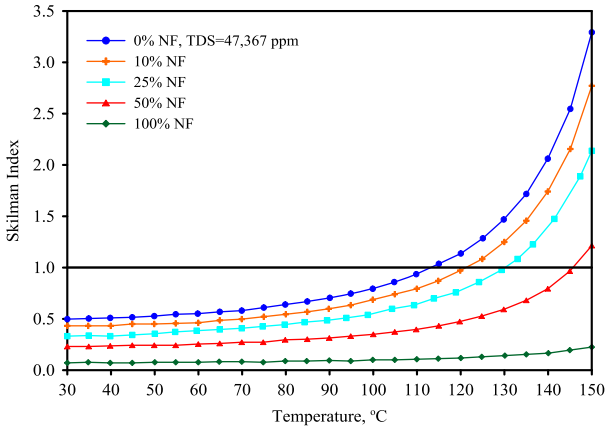

Fig. 17. Influence of NF on sulfate scale potential in BR-MSF plant [48].

stage is T_n = 40°C with 10 m^3/h distillate capacity. In this MSF, the ratio of feed (F) to distillate (D) water (F/D) is equal to:

$$\frac{F}{D} = \frac{1}{2} + \frac{L}{C(T_o - T_n)} \tag{29}$$

where L is the average latent heat between 150 and 40°C that is 2,260 kJ/kg, and C is the SW specific heat that is 4 kJ/kg°C. Therefore, F/D would be 5.64 which is as follows:

$$\frac{F}{D} = \frac{1}{2} + \frac{L}{C(T_o - T_n)} = \frac{1}{2} + \frac{2260}{4 \times (150 - 40)} = 5.635 \tag{30}$$

The gain ratio can be calculated as,

$$\mathrm{GR} = \frac{D}{S} = \left(\frac{D}{F}\right)\left(\frac{F}{S}\right) = \left(\frac{D}{F}\right)\frac{L_s}{C(T_o - t_1)} \tag{31}$$

Here, L_s is the steam latent heat at 157°C, and $(T_o - t_1)$ = 2ΔT + temperature approach in first stage (which is about $\Delta T/2$ = 1.5°C).

For 34 stages, ΔT = (150–40)/36 = 3.0, and T_o t_1 = 6.0 + 1.5= 7.5°C

$$\frac{D}{S} = \frac{1}{5.6} \times \frac{2,100}{4 \times 7.5} = 12.5 \tag{32}$$

When the unit is operated at TBT = 110°C, the expected D/S = 12.5 × (110 − 40)/(150 − 40) ≅ 8.

This means 56% increase in the gain ratio, which is the main advantage.

9.2.2. The real value of energy saving

For the OT-MSF + FO system, as a result of increasing the TBT, the heating steam will be extracted at a higher temperature compared to the conventional OT-MSF system. A rigorous analysis has been performed in order to account for the equivalent mechanical energy of the thermal energy (EMET) consumed. This analysis is based on the accounting for the availability (exergy) of the heating steam supplied to the MSF unit. This exergy represents the theoretical maximum work obtained from the steam if it is supplied to reversible Carnot heat engine cycle. When Carnot cycle receives heat from heat source at T_s (heating steam temperature to the MSF), and rejects heat to heat sink at low temperature T_c, the specific exergy of the heat supplied to the MSF unit is: W_{th}/D = (Q_b/D) $(1 - T_c/T_s)$. Here $(1 - T_c/T_s)$ is the Carnot cycle efficiency, the heat sink temperature T_c is considered, for practical reasons, the same as the power plant condenser, which is almost as T_n (brine temperature of the MSF last stage) = 40°C = 313 K. In the first case, for TBT = 110°C, if saturated steam is supplied to the MSF unit at T_s = 117°C (390 K), 7°C above TBT, T_c = 313 K, then, η(Carnot) = $(1 - T_c/T_s)$ = 19.74%, and

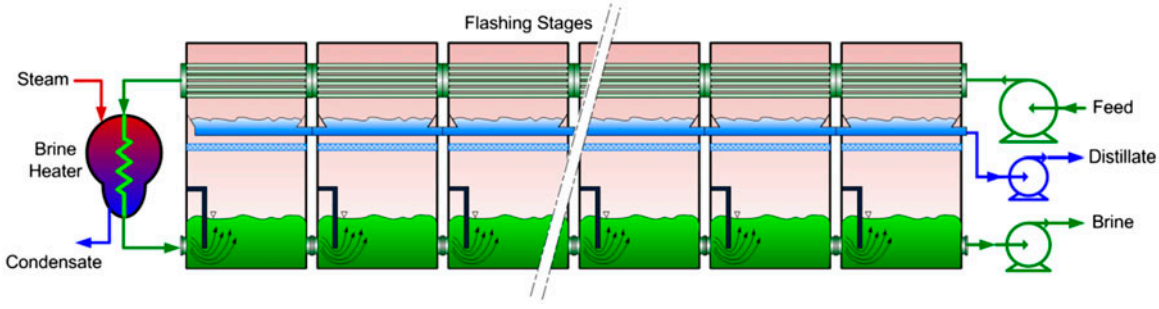

Fig. 18. Schematic diagram of OT-MSF system.

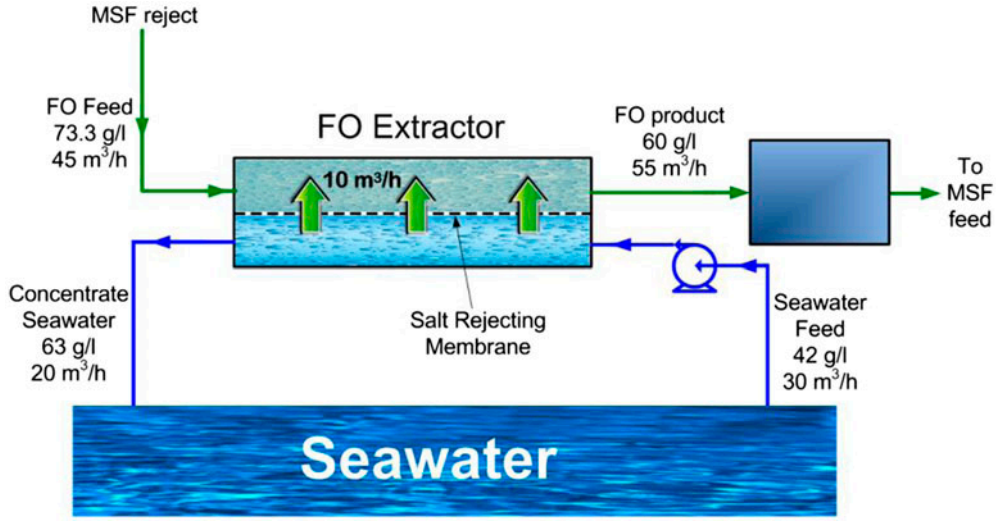

Fig. 19. Schematic diagram of the FO process with its feed supply to the MSF unit.

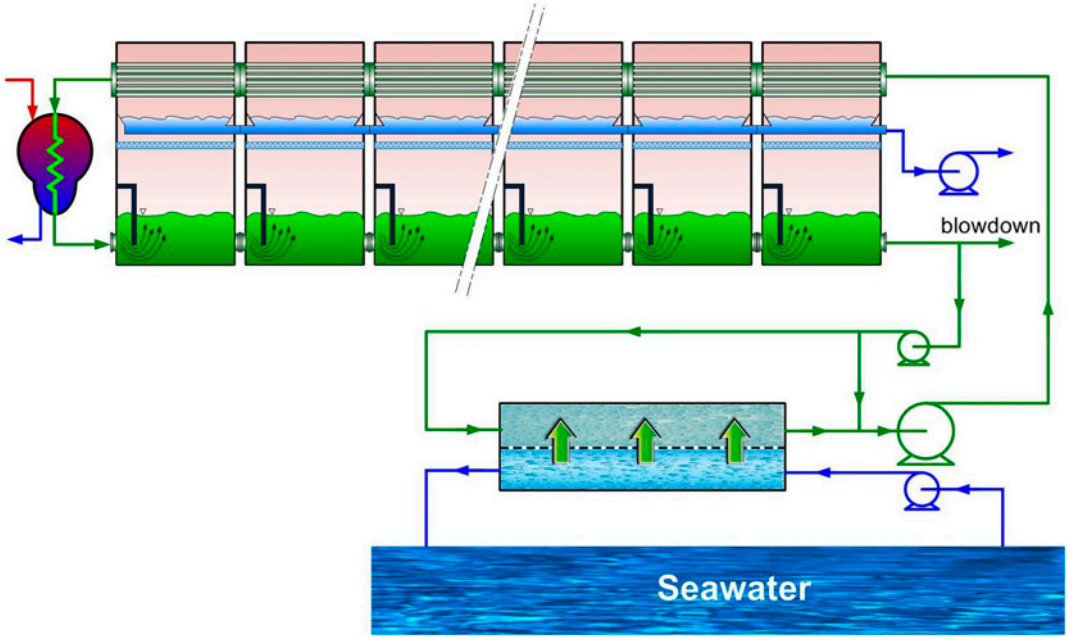

Fig. 20. Arrangement of FO as pretreatment for OT-MSF system.

theoretical specific available work output W_{th}/D is $275 \times 19.74 = 54.3$ MJ/m^3 (15.1 kWh/m^3) for $Q_b/D = 2{,}200/8 = 275$ MJ/ m^3.

In the second case, the increase in the TBT requires the increase in T_s of the heating steam temperature, and its availability. For example, if TBT = 150°C, and $T_s = 157$°C (430 K), and same $T_c = 40$°C, and $Q_b/D = 2{,}100/12.5 = 168$ MJ/m^3, then η(Carnot) = $(1 - T_c/T_s) = 1 - (313/410) = 27.21\%$, and $W_{th}/D = 45.71$ MJ/m^3 (12.7 kWh/m^3).

This means that the real effect of saving in energy in terms of mechanical energy is (54.3–45.71)/45.71 =18.8%, and not as 56% calculated from the thermal energy amount without considering the exergy of steam. However, this arrangement has several advantages:

- The application of FO unit as a pretreatment for MSF could reduce significantly the amount and temperature of brine rejected to sea, and thus

mitigates the negative impact on marine environment. Without using FO pretreatment, the volume withdrawal from sea is at least 8 times the output distillate (D), 8D, at TBT = 110°C, and the rejected to the sea is 7D at about 10°C higher temperature than SW temperature. When FO is used as a pretreatment, the volume withdrawal from sea would be 3D, and the rejected to the sea is 2D at almost the same temperature of SW. Reducing the feed flow to the MSF units reduces the pumping power consumption.

- The chemicals used for pretreatment to the MSF are significantly reduced.
- The dilution of brine reject from the MSF unit results in removing most of scale constituents, and allows for raising of the TBT and thus the GR.
- It reduces the consumed steam by the MSF.
- It reduces the scaling and fouling of the MSF system.
- It provides the benefits of FO (e.g. low energy operation and high resistance to irreversible fouling).
- Reducing operational complexities associated with using recirculation MSF system.
- Fitting the existing MSF units with FO system requires minimum system modifications.

10. Conclusions

The viability of using FO process for desalting SW is presented. The thermal energy consumed to reconcentrate the draw solution when NH_4HCO_3 solutes are used in the draw solution is more significant than the consumed mechanical energy. Development of energy-efficient draw solution recovery processes is a promising area, but these processes are still not sufficiently well established to be implemented in real systems. The use of a FO process as pretreatment for RO and MSF is a promising application. Two suggested research projects to be conducted in QEERI do not need to prepare or reconcentrate the draw solution. Dilution of the SW by TTWW significantly decreases the energy consumed by the SWRO process in the first project. In the second project, the use of FO process as pretreatment for once-through MSF raises the top brine temperature by removing the scaling constituents from SW in the FO process. Thus, it significantly raises the gain ratio, and reduces the volumes of SW intake and rejected brine. It also saves the marine environment from disposing brine of higher temperature than that of SW.

This paper also examined the FO process, and concluded that the availability of commercial FO membranes is limited and hinders the progress of the FO process. The ICP in the porous membrane support plays an important role in membrane flux reduction in FO and PRO modes, and it becomes increasingly dominant at greater draw solution concentration.

Nomenclature

A	—	transport coefficient for water (i.e. water permeability), (m/s Pa)
B	—	transport coefficient for solute (m/s)
C	—	solution concentration (M)
CP	—	concentration polarization
CTA	—	cellulose triacetate
D	—	distillate flow rate in MSF system
D	—	solute diffusion coefficient in solution (m^2/s)
ECP	—	external concentration polarization
F	—	feed flow rate in MSF
FO	—	forward osmosis
ICP	—	internal concentration polarization
J_s	—	average solute flux
J_w	—	permeate flux of water (m/s or L/m^2 h)
K	—	D/δ is the boundary-layer mass transfer coefficient, $k = \frac{Sh \cdot D}{D_h}$
K	—	solute resistivity, $K = (t \cdot \tau)/(\varepsilon \cdot D_s) = \frac{S}{D_s}$
L_s	—	steam latent heat in MSF system
P	—	applied pressure on the draw solution (Pa)
PRO	—	pressure retarded osmosis, when $\Delta\pi > \Delta P$
S	—	steam flow rate in MSF system
S	—	$\tau t/\varepsilon$ structural parameter
Sh	—	sherwood number
T	—	membrane layer thickness (m)
TBT	—	top brine temperature
T_o	—	top brine temperature
W_P	—	pump work

Greek letters

η	—	efficiency
π	—	osmotic pressure
τ	—	path tortuosity factor
ε	—	porosity of the membrane supported layer
σ	—	reflection coefficient, $\sigma = 0$ for no salt rejection, and $\sigma = 1$ for total salt rejection
δ	—	unstirred film thickness next to the dense layer, m
μ_w	—	water chemical potential (μ_w)

Subscripts

B	—	bulk stream
D	—	draw solution
F	—	feed
M	—	membrane surface
P	—	permeate
S	—	supportive layer
W	—	water

ORCID

H.K. Abdulrahim http://orcid.org/0000-0002-1223-6403

References

[1] T. Cath, A. Childress, M. Elimelech, Forward osmosis: Principles, applications, and recent developments, J. Memb. Sci. 281 (2006) 70–87.
[2] N.A. Thompson, P.G. Nicoll, Forward osmosis desalination: A commercial reality, in: World Congr. Conv. Exhib. Cent. (PCEC), Perth, Western Australia, 2011, pp. IDAWC/PER11–198.
[3] J.E. Miller, L.R. Evans, Forward Osmosis: A New Approach to Water Purification and Desalination, Sandia Natl. Lab SAND2006-4, California, CA, 2006.
[4] E.M.V. Hoek, M. Guiver, V. Nikonenko, V.V. Tarabara, A.L. Zydney, Membrane terminology, in: E.M.V. Hoek, V.V. Tarabara (Eds.), Encyclopedia of Membrane Science and Technology. Wiley, Hoboken, NJ, 2013, pp. 2219–2228.
[5] C.D. Moody, D.H. Yi, R.L. Riley, J.O. Kessler, M. Norris, Desalination by Forward Osmosis, Bur. Reclamation, 2013. Available from: http//www.usbr.gov/research/publications/download_product.cfm?id=726. Accessed January 28, 2014.
[6] S. Zhao, L. Zou, C.Y. Tang, D. Mulcahy, Recent developments in forward osmosis: Opportunities and challenges, J. Memb. Sci. 396 (2012) 1–21.
[7] Y. Xu, X. Peng, C.Y. Tang, Q.S. Fu, S. Nie, Effect of draw solution concentration and operating conditions on forward osmosis and pressure retarded osmosis performance in a spiral wound module, J. Membr. Sci. 348 (2010) 298–309.
[8] A. Tiraferri, N.Y. Yip, A.P. Straub, S. Romero-Vargas Castrillon, M. Elimelech, A method for the simultaneous determination of transport and structural parameters of forward osmosis membranes, J. Membr. Sci. 444 (2013) 523–538.
[9] Constantinos E. Salmas, George P. Androutsopoulos, A novel pore structure tortuosity concept based on nitrogen sorption hysteresis data, Ind. Eng. Chem. Res. 40 (2001) 721–730.
[10] G.T. Gray, J.R. McCutcheon, M. Elimelech, Internal concentration polarization in forward osmosis: Role of membrane orientation, Desalination 197 (2006) 1–8.
[11] S. Loeb, L. Titelman, E. Korngold, J. Freiman, Effect of porous support fabric on osmosis through a Loeb-Sourirajan type asymmetric membrane, J. Membr. Sci. 129 (1997) 243–249.
[12] Q. Ge, M. Ling, T.-S. Chung, Draw solutions for forward osmosis processes: Developments, challenges, and prospects for the future, J. Membr. Sci. 442 (2013) 225–237.
[13] T.-S. Chung, S. Zhang, K.Y. Wang, J. Su, M.M. Ling, Forward osmosis processes: Yesterday, today and tomorrow, Desalination 287 (2012) 78–81.
[14] R.A. Neff, Solvent extractor. US Patent: 3130156, 1964.
[15] J.R. McCutcheon, R.L. McGinnis, M. Elimelech, Desalination by ammonia–carbon dioxide forward osmosis: Influence of draw and feed solution concentrations on process performance, J. Membr. Sci. 278 (2006) 114–123.
[16] R.L. McGinnis, J.R. McCutcheon, M. Elimelech, A novel ammonia–carbon dioxide osmotic heat engine for power generation, J. Membr. Sci. 305 (2007) 13–19.
[17] J.R. McCutcheon, R.L. McGinnis, M. Elimelech, A novel ammonia–carbon dioxide forward (direct) osmosis desalination process, Desalination 174 (2005) 1–11.
[18] A. Achilli, T.Y. Cath, A.E. Childress, Selection of inorganic-based draw solutions for forward osmosis applications, J. Membr. Sci. 364 (2010) 233–241.
[19] G.W. Batchelder, Process for the demineralization of water. US Patent 3171799, 1965.
[20] D.N. Glew, Process for liquid recovery and solution concentration. US Patent 3216930, 1965.
[21] R.L. McGinnis, Osmotic desalination process. US Patent 6391205 B1, 2002.
[22] J.R. Herron, E.G. Beaudry, C.E. Jochums, L.E. Medina, Osmotic concentration apparatus and method for direct osmotic concentration of fruit juices. US Patent 5281430, 1994.
[23] J.C. Su, T.S. Chung, B.J. Helmer, J.S. de Wit, Enhanced double-skinned FO membranes with inner dense layer for wastewater treatment and macromolecule recycle using Sucrose as draw solute, Membr. Sci. 396 (2012) 92–100.
[24] R.E. Kravath, J.A. Davis, Desalination of seawater by direct osmosis, Desalination 16 (1975) 151–155.
[25] J.O. Kessler, C.D. Moody, Drinking water from sea water by forward osmosis, Desalination 18 (1976) 297–306.
[26] K. Stache, Apparatus for transforming seawater, Brackish water, polluted water or the like into a nutritious drink by means of osmosis. US Patent 4879030 A, 1989.
[27] J. Yaeli, Method and apparatus for processing liquid solutions of suspensions particularly useful in the desalination of saline water. US Patent 5098575 A, 1992.
[28] E. Barbera, Experimental Investigation of Sugar Aqueous Solutions Separation by Reverse Osmosis for the Manipulated Osmosis Desalination Process, Università Degli Studi Di Padova, 2013. Available from: http://tesi.cab.unipd.it/44538/1/Master_thesis_-_Elena_Barbera.pdf.
[29] B.S. Frank, Desalination of sea water. US Patent 3670897 A, 1972.
[30] A. Altaee, A. Mabrouk, K. Bourouni, A novel Forward osmosis membrane pretreatment of seawater for thermal desalination processes, Desalination 326 (2013) 19–29.
[31] Q. Saren, C.Q. Qiu, C.Y. Tang, Synthesis and characterization of novel Forward osmosis membranes based on layer-by-layer assembly, Environ. Sci. Technol. 45 (2011) 5201–5208.
[32] B.D. Coday, The effect of trans-membrane hydraulic performance of forwards osmosis membranes. MSc degree, Civil and Environmental Engineering, Colorado School of Mines, Colorado, CO, 2013.
[33] A. Mabrouk, Technoeconomic analysis of once through long tube MSF process for high capacity desalination plants, Desalination 317 (2013) 84–94.
[34] R. Wang, L. Shi, C.Y. Tang, S. Chou, C. Qiu, A.G. Fane, Characterization of novel forward osmosis hollow fiber membranes, J. Membr. Sci. 355 (2010) 158–167.

[35] R. Semiat, J. Sapoznik, D. Hasson, Energy Aspects in Osmotic Processes, Desalin. Water Treat. 15 (2010) 228–235.
[36] G. Danasamy, Sustainability of seawater desalination technology—the study of forward osmosis as a new alternative. MSc, Imperial College, London, 2009.
[37] T. Kim, S. Park, K. Yeh, Cost-effective design of a draw solution recovery process for forward osmosis desalination, Desalination 327 (2013) 46–51.
[38] M.F. Flanagan, Polybenzimidazole membranes functionalized to increase hydrophilicity, increase surface charge, and reduce pore size for forward osmosis applications. MSc, The University of Toledo, Toledo, OH, 2012.
[39] Z.-Y. Li, V. Yangali-Quintanilla, R. Valladares-Linares, Q. Li, T. Zhan, G. Amy, Flux patterns and membrane fouling propensity during desalination of seawater by forward osmosis, Water Res. 46 (2012) 195–204.
[40] R.L. McGinnis, M. Elimelech, Energy requirements of ammonia–carbon dioxide forward osmosis desalination, Desalination 207 (2007) 370–382.
[41] P.G. Nicoll, Forward osmosis as pretreatment to reverse osmosis, in: Int. Desalin. Assoc. World Congr. Desalin. Water Reuse, Tianjin, China, REF IDAWC/TIAN13-318, 2013.
[42] S. Lee, C. Boo, M. Elimelech, S. Hong, Comparison of fouling behavior in forward osmosis (FO) and reverse osmosis (RO), J. Membr. Sci. 365 (2010) 34–39.
[43] T.Y. Cath, J.E. Drewes, C.D. Lundin, A Novel Hybrid Forward Osmosis Process for Drinking Water Augmentation using Impaired Water and Saline Water Sources, WERC, a Consortium for Environmental Education and Technology Development at New Mexico State University, Water Research Foundation, Las Cruces, New Mexico, 2009.
[44] M. Darwish, Thermal desalination in GCC and possible development, Desalin. Water Treat. 52 (2014) 27–47.